Alternating Minimization Algorithms for X-Ray CT Imaging

Joseph A. O'Sullivan

Electronic Systems and Signals Research Laboratory
Department of Electrical and Systems Engineering
Washington University
jao@wustl.edu
http://essrl.wustl.edu/~jao

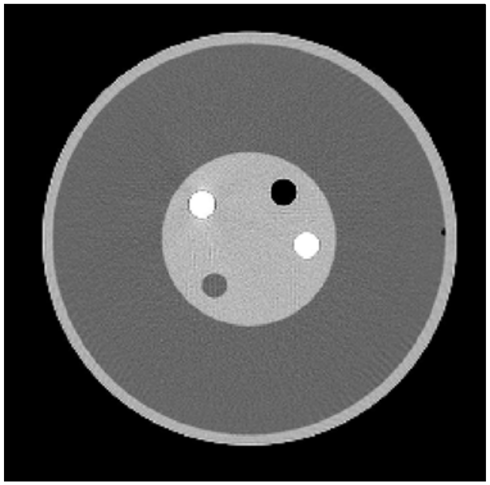

Presented to VCU University Radiation Oncology, March 31, 2004.

Supported by: NIH grant R01CA75371 from the National Cancer Institute (J. F. Williamson, VCU, PI).

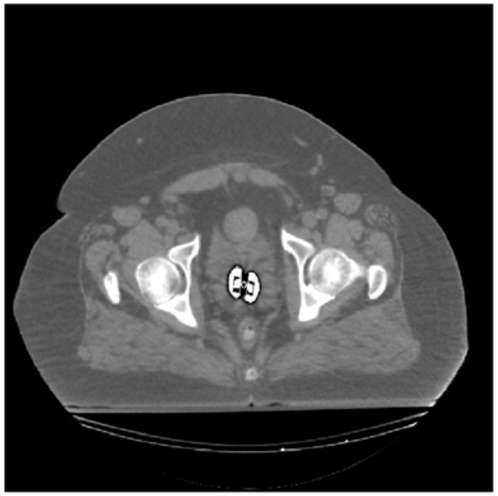

Collaborators

Faculty

Donald L. Snyder
Jeffrey F. Williamson, VCU
Bruce R. Whiting
David G. Politte
G. James Blaine

Students

Ryan Murphy
Jasenka Benac
Shenyu Yan
Orville Earl

Outline

- X-Ray CT
  - Transmission Tomography
  - Maximum Likelihood Viewpoint
  - General Problem
- Alternating Minimization Algorithms
  - Information Geometry
  - Projections of I-Divergence
- X-Ray CT
  - Phantom Experiments
  - Physical Considerations
  - Extensions
- Conclusions

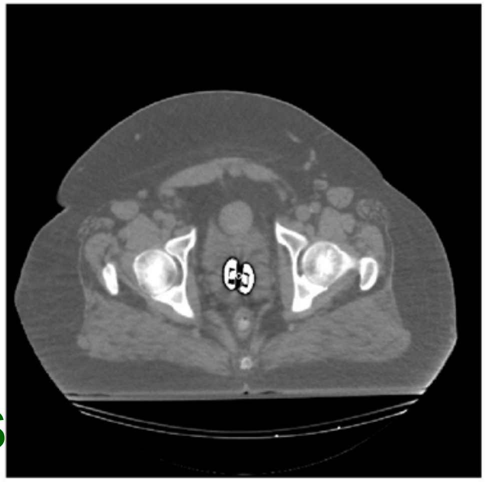

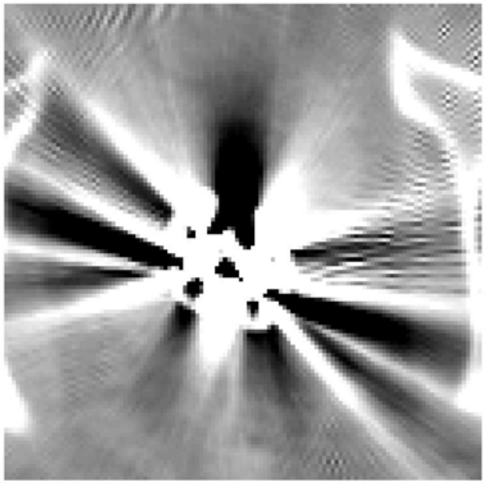

Outline

- X-Ray CT
  - Transmission Tomography
  - Maximum Likelihood Viewpoint
  - General Problem
- Alternating Minimization Algorithms
  - Information Geometry
  - Projections of I-Divergence
- X-Ray CT
  - Phantom Experiments
  - Physical Considerations
  - Extensions
- Conclusions

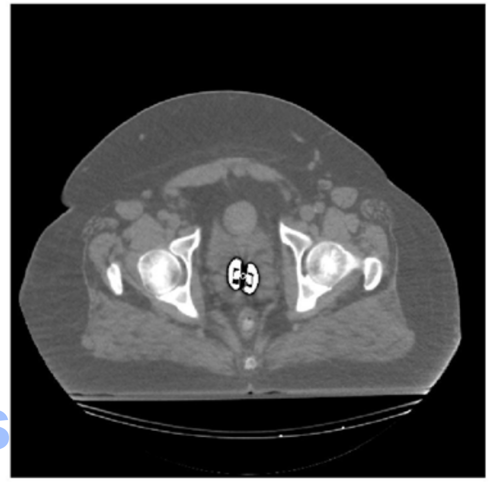

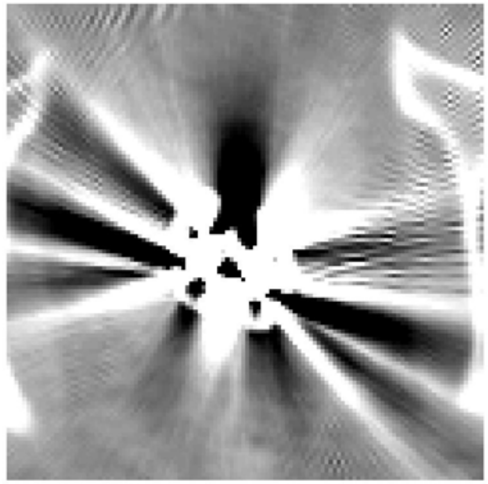

CT Imaging in Presence of High Density Attenuators

Brachytherapy applicators
After-loading colpostats
for radiation oncology

Cervical cancer: 50% survival rate
Dose prediction important

Object-Constrained Computed Tomography (OCCT)

Filtered Back Projection

FBP: inverse Radon transform

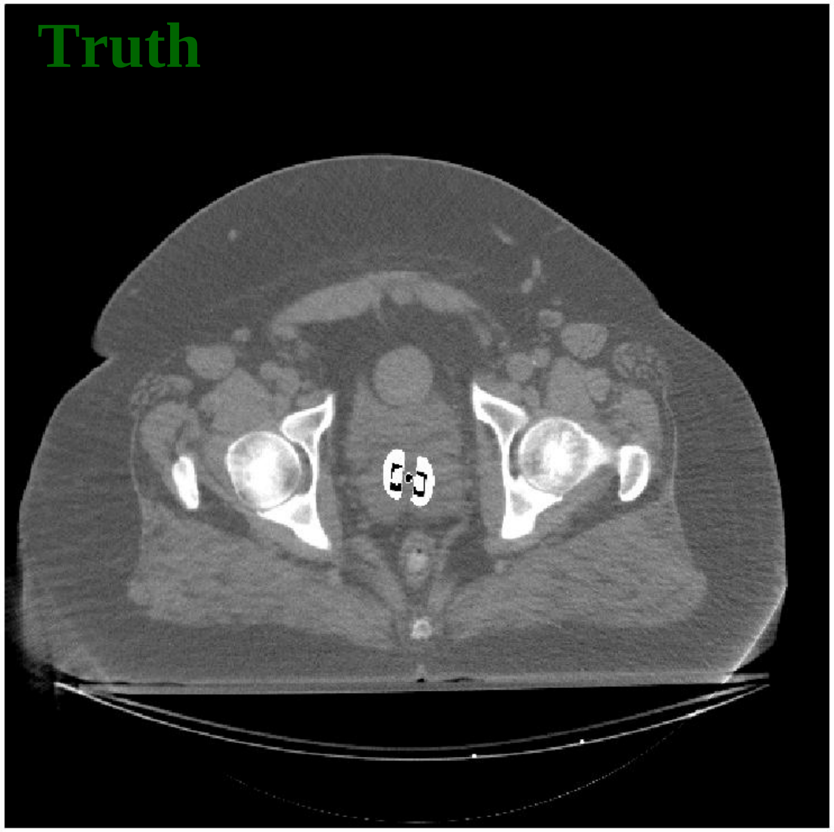

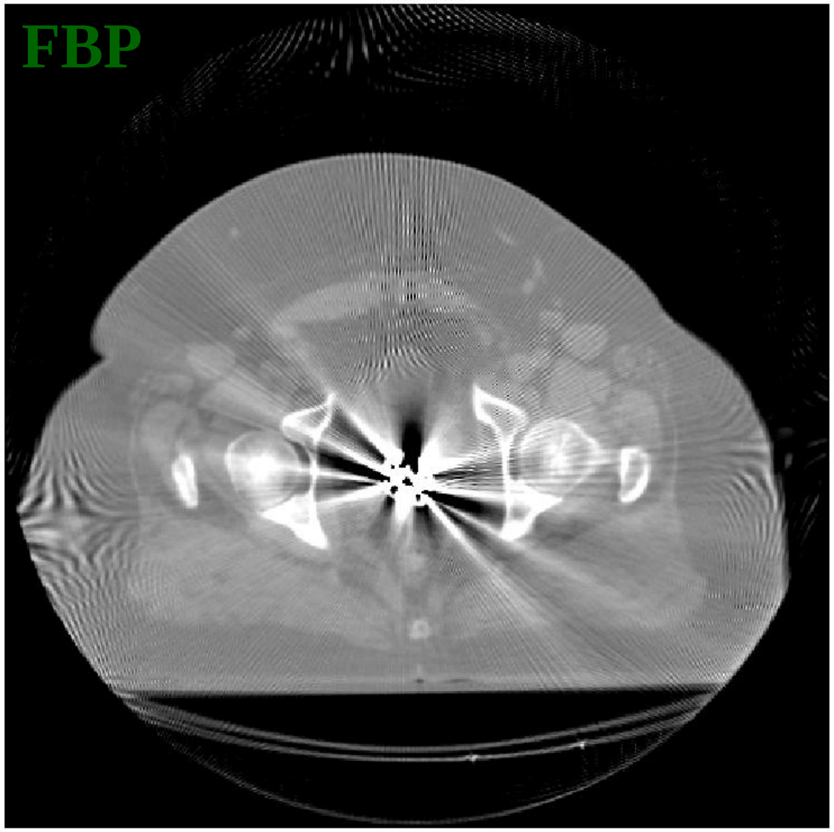

Transmission Tomography

- **Source-detector pairs indexed by *y*; pixels indexed by *x***
- **Data *d(y)* Poisson, means *g(y:*μ*)*, log likelihood function**

$$l(d \mid g(\cdot:\mu)) = \sum_{y \in Y} d(y) \ln g(y:\mu) - g(y:\mu)$$

$$g(y:\mu) = \sum_{E} I_0(y,E) \exp\left(-\sum_{x \in X} h(y,x)\mu(x,E) \right) + \beta(y)$$

- **Mean unattenuated counts I_0, mean background β**

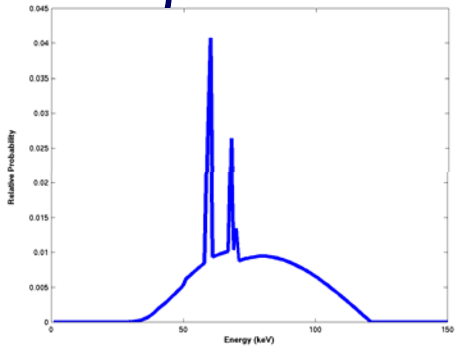

- **Attenuation function μ*(x,E)*, *E* energies**

$$\mu(x,E) = \sum_{i=1}^{I} c_i(x)\mu_i(E)$$

- **Maximize over μ or c_i; equivalently minimize I-divergence**

Maximum-Likelihood → Minimum I-divergence

- **Poisson distribution**

$$P(N=k)=\frac{\lambda^k}{k!}e^{-\lambda}$$

- **Poisson distributed data → loglikelihood function**

$$\ln P(N=k)=k\ln\lambda-\lambda-\ln k!$$

$$I(k\,\|\,\lambda)=k\ln\frac{k}{\lambda}-k+\lambda$$

- **Maximization over μ equivalent to minimization of I-divergence**

$$l(d\,|\,g(\cdot:\mu))=\sum_{y\in\mathrm{Y}}d(y)\ln g(y:\mu)-g(y:\mu)$$

$$I(d\,\|\,g(\cdot:\mu))=\sum_{y\in\mathrm{Y}}d(y)\ln\frac{d(y)}{g(y:\mu)}-d(y)+g(y:\mu)$$

$$g(y:\mu)=\sum_{E}I_0(y,E)\exp\left(-\sum_{x\in\mathrm{X}}h(y,x)\mu(x,E)\right)+\beta(y)$$

Maximum Likelihood → Minimum I-Divergence

$$l(d \mid g(\cdot : \mu)) = \sum_{y \in \mathrm{Y}} d(y) \ln g(y : \mu) - g(y : \mu)$$

$$I(d \,\|\, g(\cdot : \mu)) = \sum_{y \in \mathrm{Y}} d(y) \ln \frac{d(y)}{g(y : \mu)} - d(y) + g(y : \mu)$$

$$g(y : \mu) = \sum_{E} I_0(y, E) \exp\left(- \sum_{x \in \mathrm{X}} h(y, x) \sum_{i=1}^{I} c_i(x) \mu_i(E) \right) + \beta(y)$$

Difficulties: log of sum, sums in exponent

Outline

- X-Ray CT
  - Transmission Tomography
  - Maximum Likelihood Viewpoint
  - General Problem
- Alternating Minimization Algorithms
  - Information Geometry
  - Projections of I-Divergence
- X-Ray CT
  - Phantom Experiments
  - Physical Considerations
  - Extensions
- Conclusions

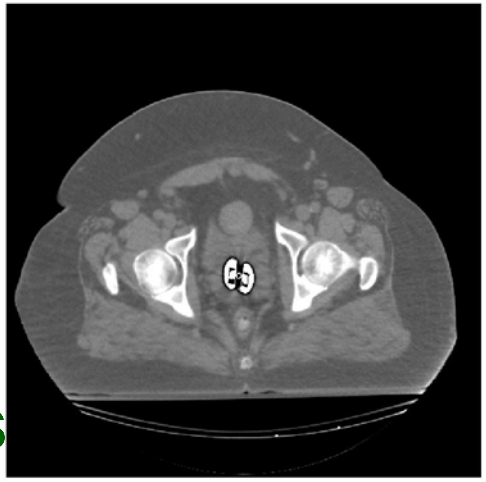

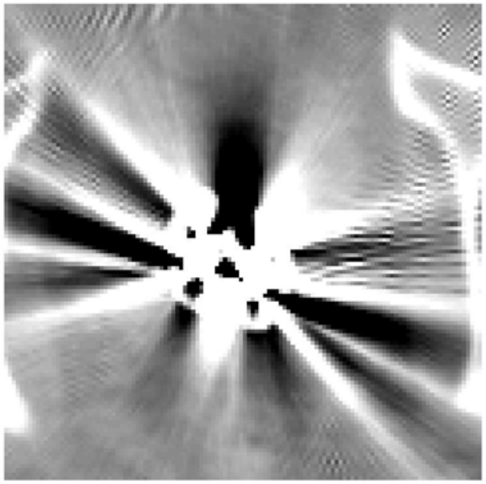

Information Geometry: Properties of I-Divergence

$$I(p\,\|\,q) = \sum_i p_i \ln\frac{p_i}{q_i} - p_i + q_i$$

- **I-divergence is nonnegative, convex in pair *(p,q)***
- **Generalization of relative entropy; not symmetric; example of f-divergence (Csiszár)**
- **Let *P* be a probability matrix. Then**

$$I(Pp\,\|\,Pq) \le I(p\,\|\,q)$$

- **First projection property**

$$A = \sum_i p_i \quad B = \sum_i q_i$$

$$I(p\,\|\,q) = I(A\,\|\,B) + A I(p/A\,\|\,q/B)$$

Variational Representations

- **Convex Decomposition Lemma.**

$$\ln\left(\sum_i q_i\right) = -\min_{p\in\mathcal{P}} \sum_i p_i \ln\frac{p_i}{q_i}$$

$$\mathcal{P} = \left\{ p : p_i \geq 0, \sum_i p_i = 1 \right\}$$

- **Basis for EM; see also De Pierro, Lange, Fessler**

$$\ln[g(y:\mu)] = \ln\left[\sum_E I_0(y,E)\exp\left(-\sum_{x\in\mathcal{X}} h(y,x)\sum_{i=1}^{I} c_i(x)\mu_i(E)\right)\right]$$

$$= \min_{p\in\mathcal{L}} \sum_E p(y,E)\ln\frac{p(y,E)}{q(y,E)}$$

$$q(y,E) = I_0(y,E)\exp\left(-\sum_{x\in\mathcal{X}} h(y,x)\sum_{i=1}^{I} c_i(x)\mu_i(E)\right)$$

Information Geometry: Projections Using I-Divergence

- Define the linear family

$$\mathcal{L}(A,b) = \left\{ p \in \Re_+^n : Ap = b \right\}$$

- **Theorem.** Suppose that *q* and L are given. Let *p** in L achieve

$$p^* = \arg\min_{p \in \mathcal{L}(A,b)} I(p \,\|\, q)$$

then for all *p* in L

$$I(p \,\|\, q) = I(p \,\|\, p^*) + I(p^* \,\|\, q)$$

Information Geometry: Projections Using I-Divergence

- **Define the exponential family**

$$\mathrm{E}\,(\pi, B) = \left\{ q \in \Re_{+}^{n} : q_i = \pi_i \exp\left(\sum_k b_{ki} \nu_k \right), \text{for some } \nu \right\}$$

- **Theorem. Suppose that *p* and E are given. Let q* in E achieve**

$$q^{*} = \arg\min_{q \in \mathrm{E}\,(\pi, B)} I(p \,\|\, q)$$

- **then for all *q* in *E* ,**

$$I(p \,\|\, q) = I(p \,\|\, q^{*}) + I(q^{*} \,\|\, q)$$

Comment on Proofs

Duality Theorem: the two problems below are (Fenchel) dual, with solutions *q* = p*.*

$$\min_{q \in \mathcal{E}(\pi, B)} I(d \| q)$$

$$\min_{p \in \mathcal{L}(B^T, B^T d)} I(p \| \pi)$$

The resulting values of the objective functions satisfy

$$I(d \| \pi) = I(d \| q^*) + I(q^* \| \pi)$$

More Information Geometry…

- Shun-ichi Amari, Imre Csiszár
- Two types of information geodesics:
  - Linear, m-projections
  - Exponential, e-projections
- Differential geometry on manifold of probability density functions
- Fisher Information is the Riemannian metric
- Exponential family → e-flat manifold → dually flat Riemannian space
- Dual parameterization: mean and exponential family parameter

Alternating Minimization Algorithms

- **Define problem as min$_q$ ϕ*(q)***
- **Derive variational representation: ϕ*(q)* = min$_p$ *J(p,q)***
- ***J* is an auxiliary function; *p* is in auxiliary set *P***
- **Result: double minimization min$_q$ min$_p$ *J(p,q)***
- **Alternating minimization algorithm**

$$p^{(l+1)} = \arg\min_{p \in P} J(p, q^{(l)})$$

$$q^{(l+1)} = \arg\min_{q \in Q} J(p^{(l+1)}, q)$$

Comments: Guaranteed Monotonicity; *J* selected carefully

Alternating Minimization Algorithms: I-Divergence, Linear, Exponential Families

- **Special Case of Interest: *J* is I-divergence**
- **Families of Interest:**
Linear Family *L(A,b) = {p: Ap = b}*
Exponential Family *E(π,B) = {q: $q_i = \pi_i \exp[\Sigma_j b_{ij} \nu_j]$}*

$$p^{(l+1)} = \arg\min_{p \in \mathrm{L}(A,b)} I(p \,\|\, q^{(l)})$$

$$q^{(l+1)} = \arg\min_{q \in \mathrm{E}(\pi,B)} I(p^{(l+1)} \,\|\, q)$$

Csiszár and Tusnády; Dempster, Laird, Rubin; Blahut; Richardson; Lucy; Vardi, Shepp, and Kaufman; Cover; Miller and Snyder; O'Sullivan

Alternating Minimization Example

- **Linear family: $p_1 + 2\,p_2 = 2$**
- **Exponential family: $q_1 = \exp(v)$, $q_2 = \exp(-v)$**

$$\min_{q \in E} \min_{p \in L} I(p \,\|\, q)$$

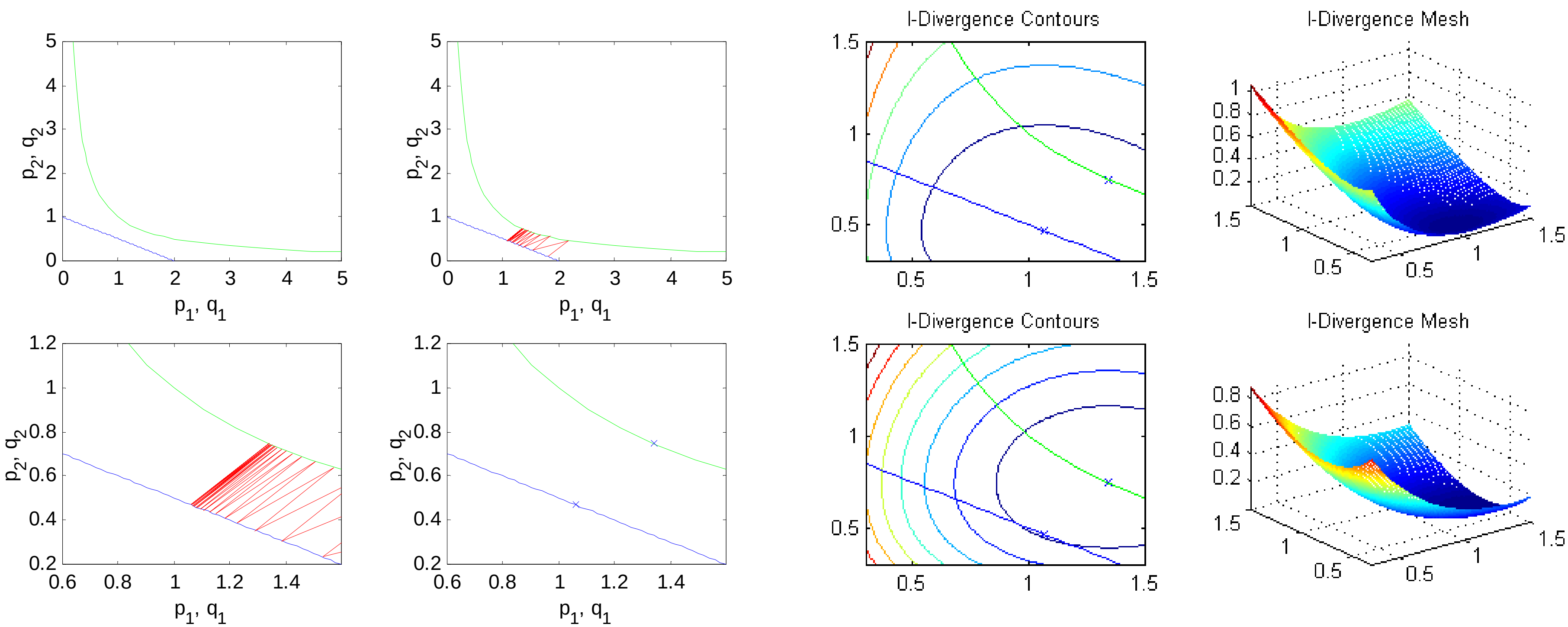

Alternating Minimization Algorithms

- **Projections and triangle equality**

$$I(p^{(l)} \| q^{(l)}) = I(p^{(l)} \| p^{(l+1)}) + I(p^{(l+1)} \| q^{(l)})$$

$$I(p^{(l+1)} \| q^{(l)}) = I(p^{(l+1)} \| q^{(l+1)}) + I(q^{(l+1)} \| q^{(l)})$$

- **Bounded sums (depending on initial condition)**

$$\sum_{l=1}^{\infty} I(p^{(l)} \| p^{(l+1)})$$

$$\sum_{l=1}^{\infty} I(q^{(l+1)} \| q^{(l)})$$

- **Monotonicity; limit points exist, form connected set**

New Alternating Minimization Algorithm for Transmission Tomography

$$\min_{q} \min_{p \in \mathcal{L}} I(p \| q) = \sum_{y \in \mathcal{Y}} \sum_{E} p(y,E) \ln \frac{p(y,E)}{q(y,E)} - p(y,E) + q(y,E)$$

$$q(y,E) = I_0(y,E) \exp\left(-\sum_{x \in \mathcal{X}} h(y,x) \sum_{i=1}^{I} c_i(x) \mu_i(E) \right)$$

$$\mathcal{L} = \left\{ p(y,E) : \sum_{E} p(y,E) = d(y) \right\}$$

Data determine the linear family
Exponential family parameters are image(s)

Alternating Minimization Algorithm

Image update

$$\hat{c}_i^{(l+1)}(x) = \hat{c}_i^{(l)}(x) - \frac{1}{Z_i(x)} \ln \frac{\tilde{b}_i^{(l)}(x)}{\hat{b}_i^{(l)}(x)}$$

Interpretation:

- compare predicted data to measured data via ratio of backprojections
- update estimate using a normalization constant

$$\tilde{b}_i^{(l)}(x) = \sum_y \sum_E \mu_i(E) h(y,x) \hat{p}^{(l)}(y,E)$$

$$\hat{b}_i^{(l)}(x) = \sum_y \sum_E \mu_i(E) h(y,x) \hat{q}^{(l)}(y,E)$$

Alternating Minimization Algorithm
Image update

$$\hat{c}_i^{(l+1)}(x) = \hat{c}_i^{(l)}(x) - \frac{1}{Z_i(x)} \ln \frac{\tilde{b}_i^{(l)}(x)}{\hat{b}_i^{(l)}(x)}$$

Interpretation:

- compare predicted data to measured data via ratio of backprojections
- update estimate using a normalization constant

Comments:

- choice for constants
- monotonic convergence
- constraints easily incorporated
- computationally expensive:

  N forward, 2 *N* backward projections per iteration

Derivation of Iterations

$$\min_q \min_{p \in \mathcal{L}} I(p \| q) = \sum_{y \in \mathcal{Y}} \sum_E p(y,E) \ln \frac{p(y,E)}{q(y,E)} - p(y,E) + q(y,E)$$

$$q(y,E) = I_0(y,E) \exp\left(-\sum_{x \in \mathcal{X}} h(y,x) \sum_{i=1}^{I} c_i(x) \frac{Z_i(x)}{Z_i(x)} \mu_i(E) \right) \leq$$

$$I_0(y,E) \exp\left(-\sum_{x \in \mathcal{X}} h(y,x) \sum_{i=1}^{I} c_i^{(k)}(x) \mu_i(E) \right) \sum_{x \in \mathcal{X}} \sum_{i=1}^{I} \frac{h(y,x)\mu_i(E)}{Z_i(x)} \exp\left(-Z_i(x) \Delta c_i^{(k+1)}(x) \right)$$

$$I(p^{(k)} \| q) \leq \sum_{x \in \mathcal{X}} \sum_{i=1}^{I} \tilde{b}_i(x) \left[c_i^{(k)}(x) + \Delta c_i^{(k+1)}(x) \right] + \hat{b}_i(x) \frac{1}{Z_i(x)} \exp\left(-Z_i(x) \Delta c_i^{(k+1)}(x) \right)$$

$$+ \text{other terms}$$

Outline

- X-Ray CT
  - Transmission Tomography
  - Maximum Likelihood Viewpoint
  - General Problem
- Alternating Minimization Algorithms
  - Information Geometry
  - Projections of I-Divergence
- X-Ray CT
  - Phantom Experiments
  - Physical Considerations
  - Extensions
- Conclusions

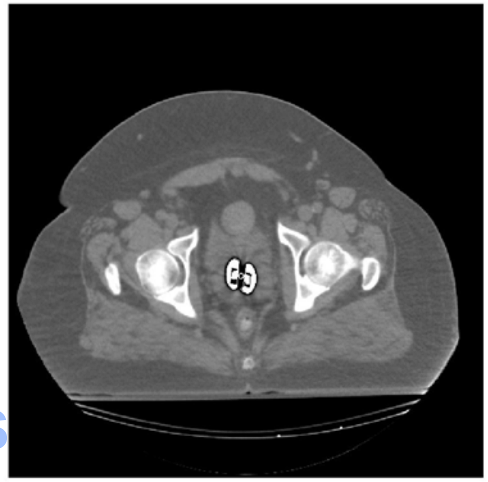

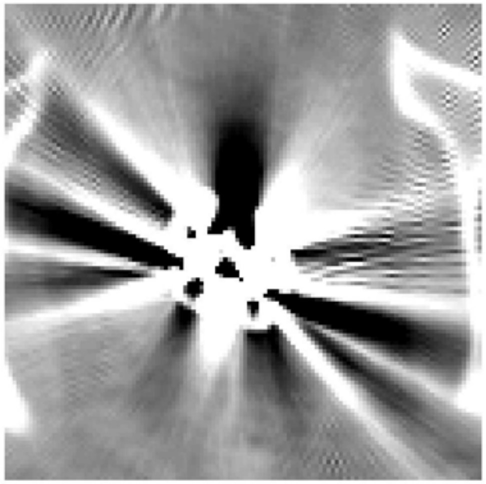

Mini CT, AM Iteration 0000001

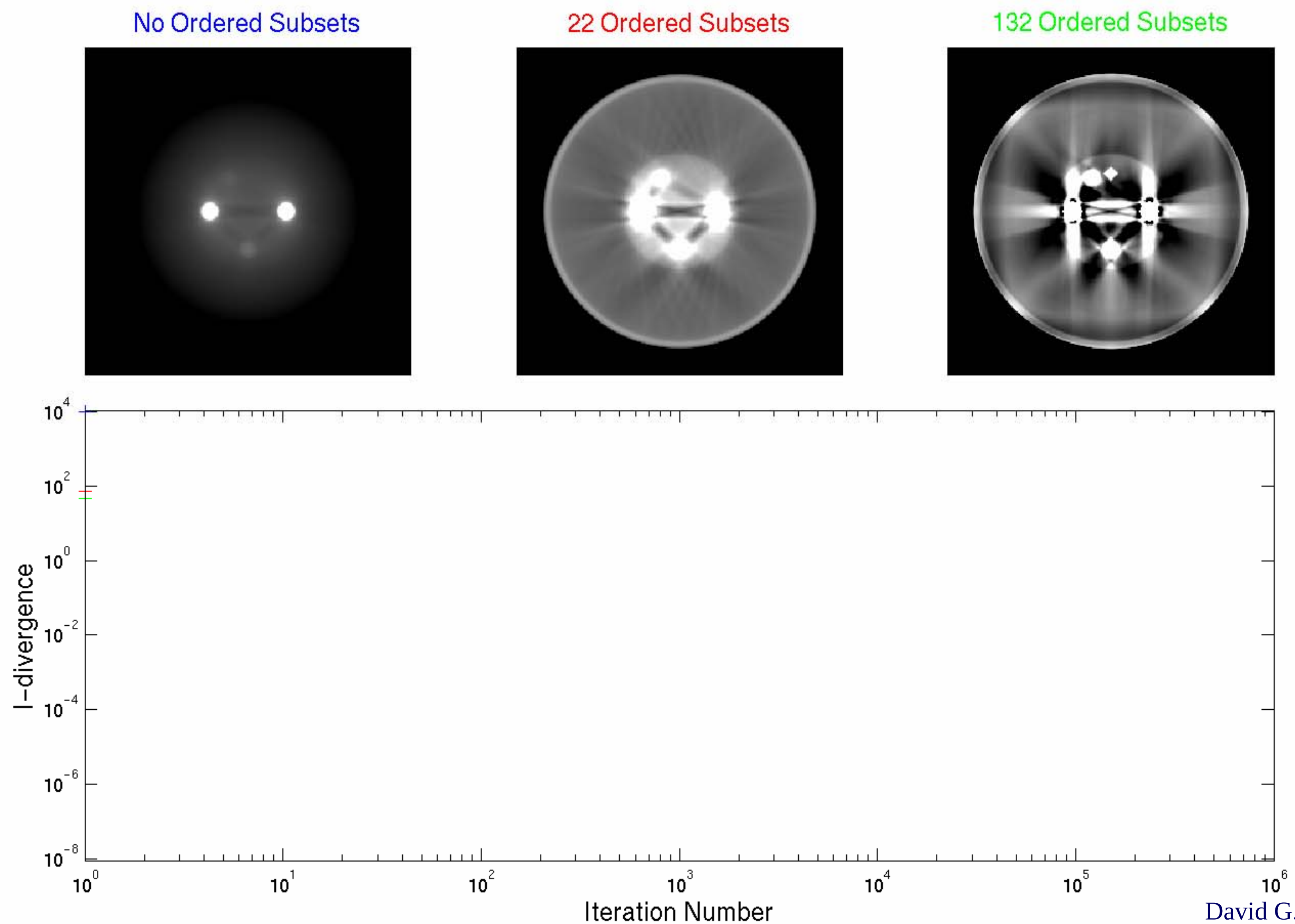

David G. Politte
October 31, 2002

Mini CT, AM Iteration 0000002

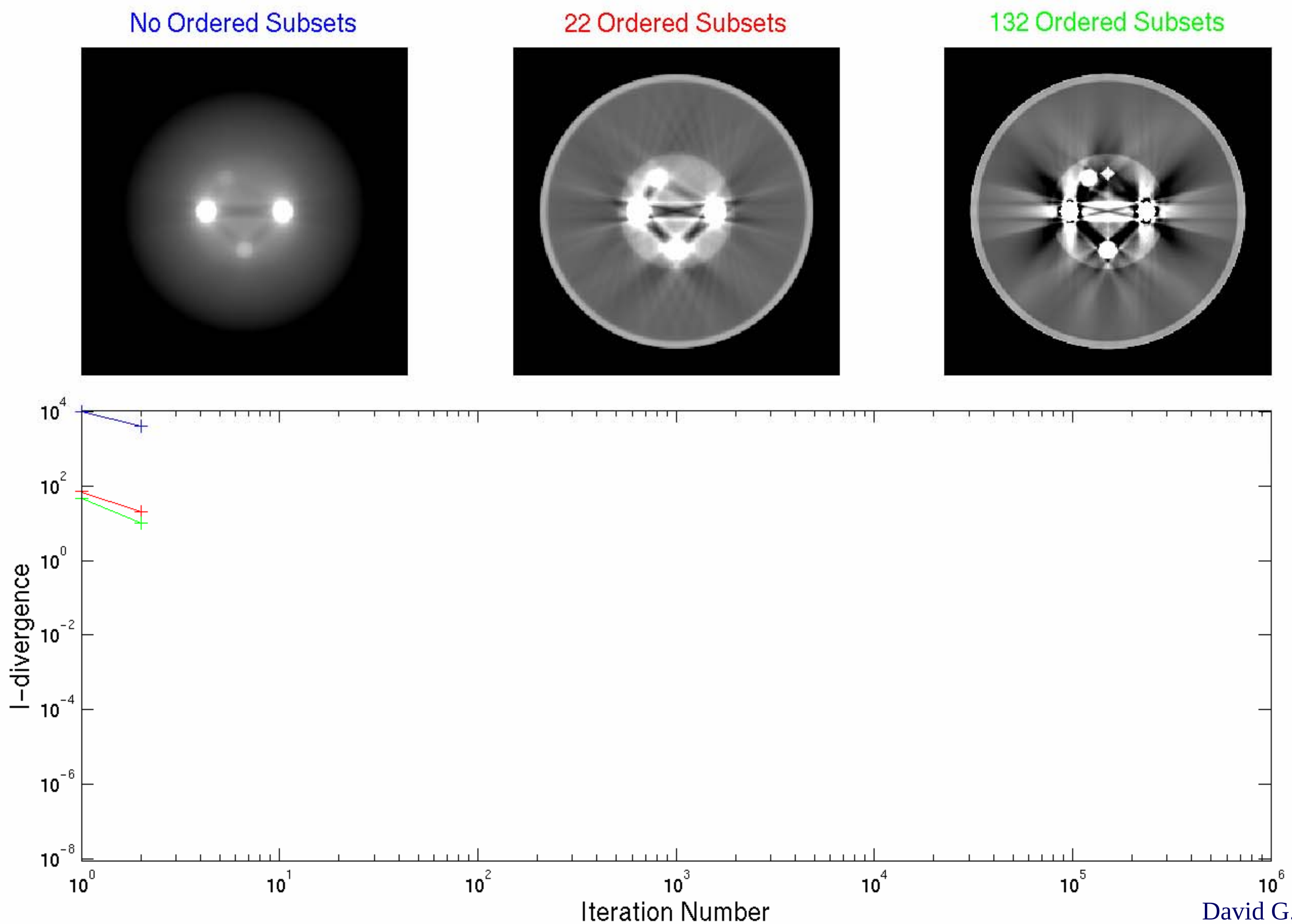

David G. Politte
October 31, 2002

Mini CT, AM Iteration 0000005

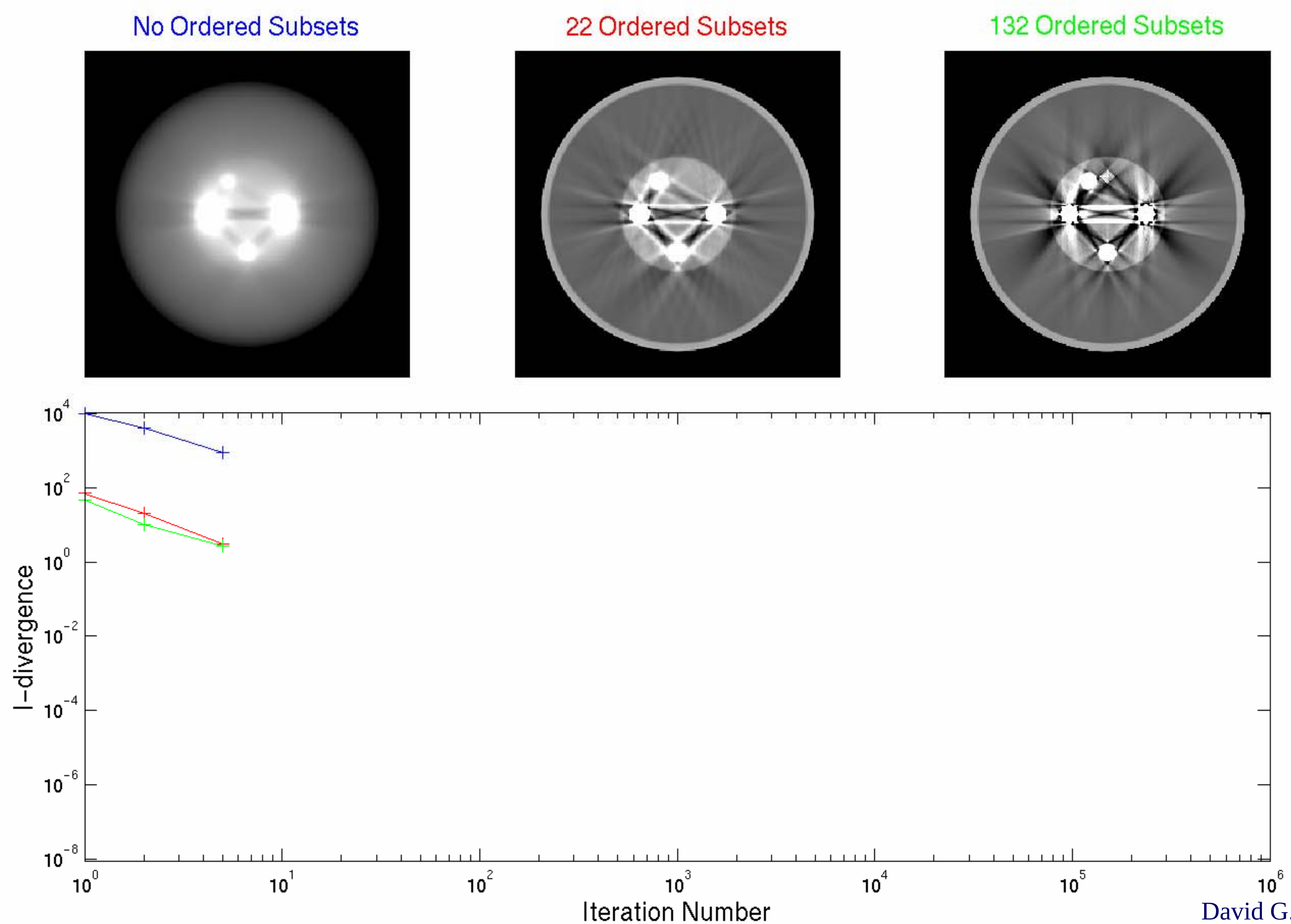

David G. Politte
October 31, 2002

Mini CT, AM Iteration 0000010

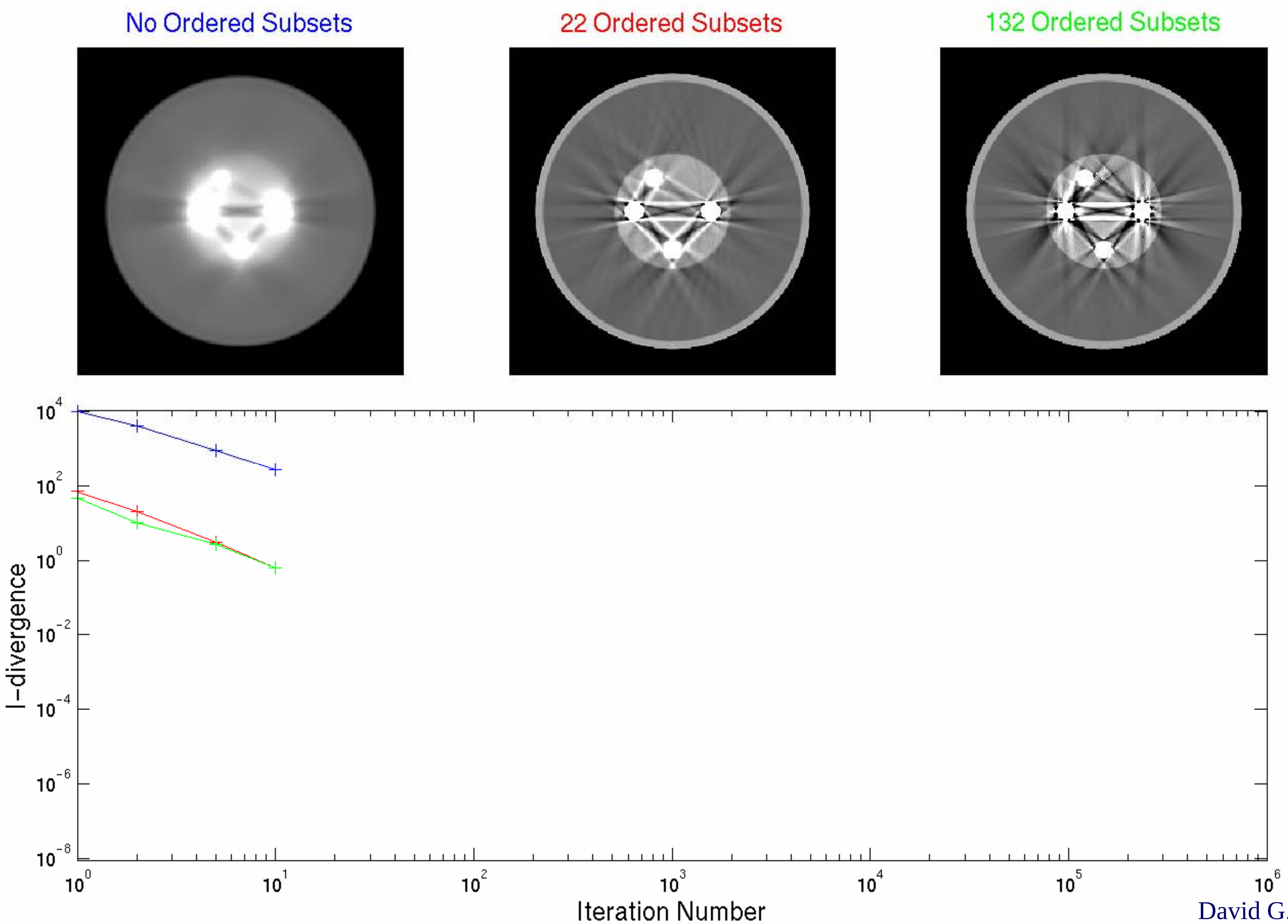

David G. Politte
October 31, 2002

Mini CT, AM Iteration 0000020

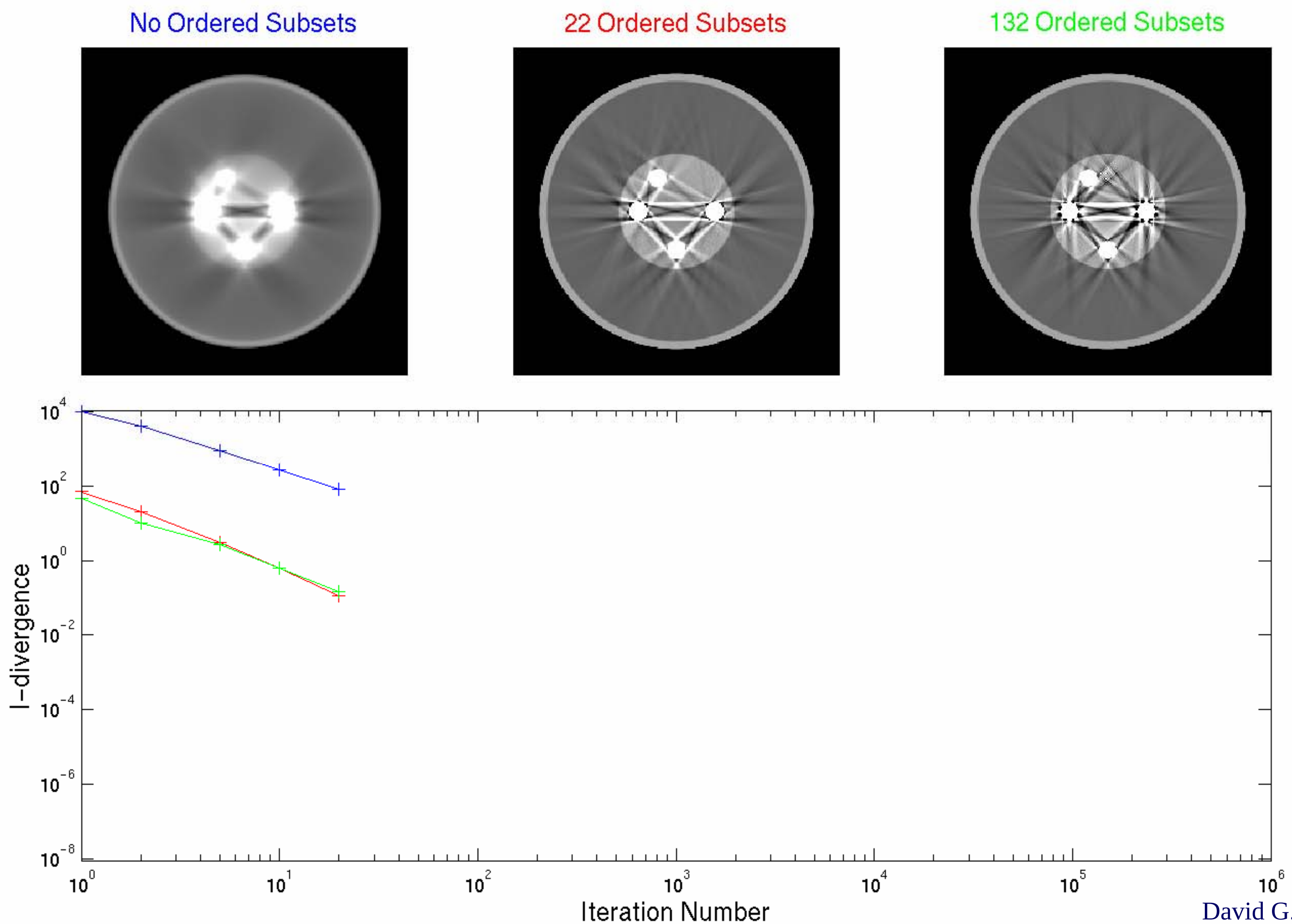

David G. Politte
October 31, 2002

Mini CT, AM Iteration 0000050

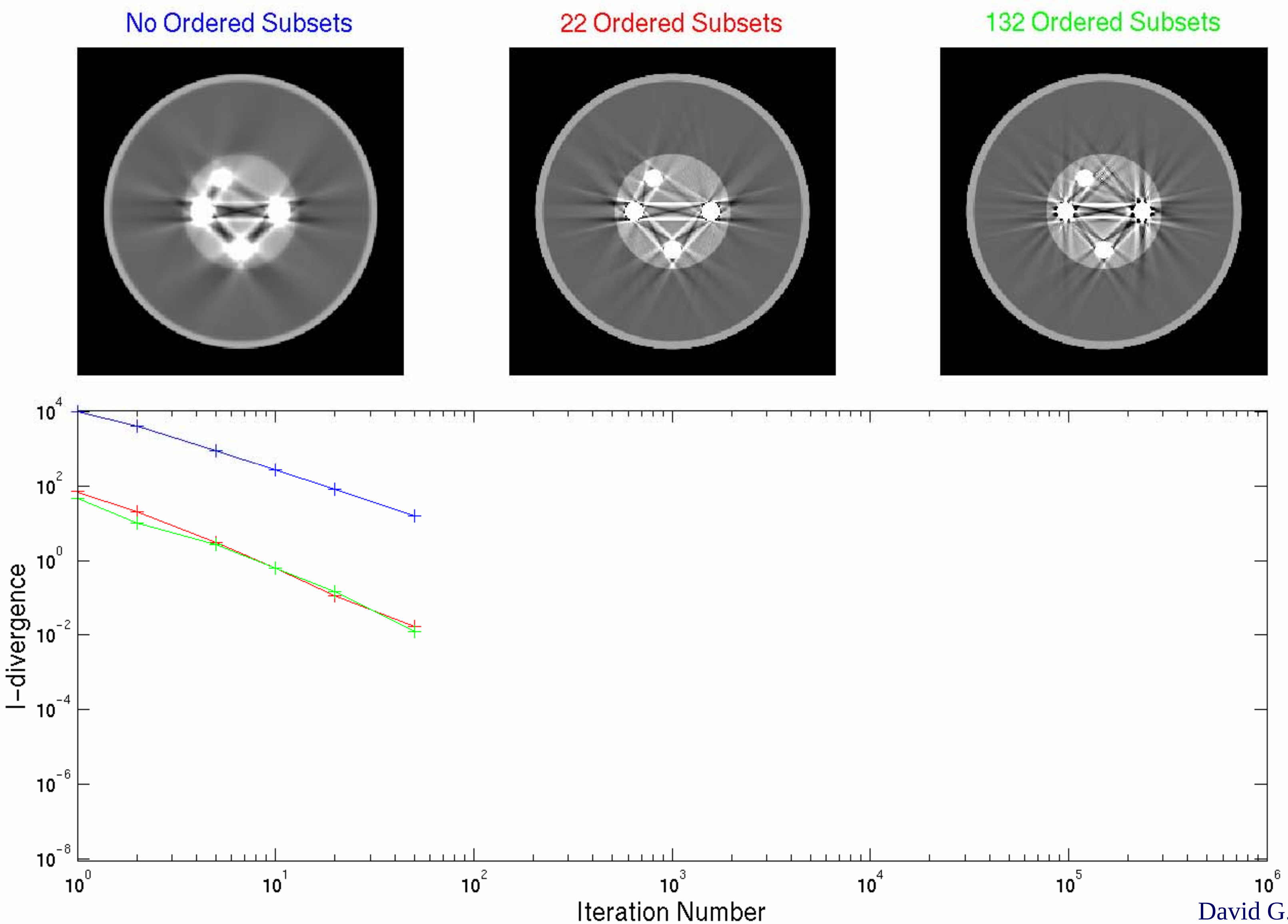

David G. Politte
October 31, 2002

Mini CT, AM Iteration 0000100

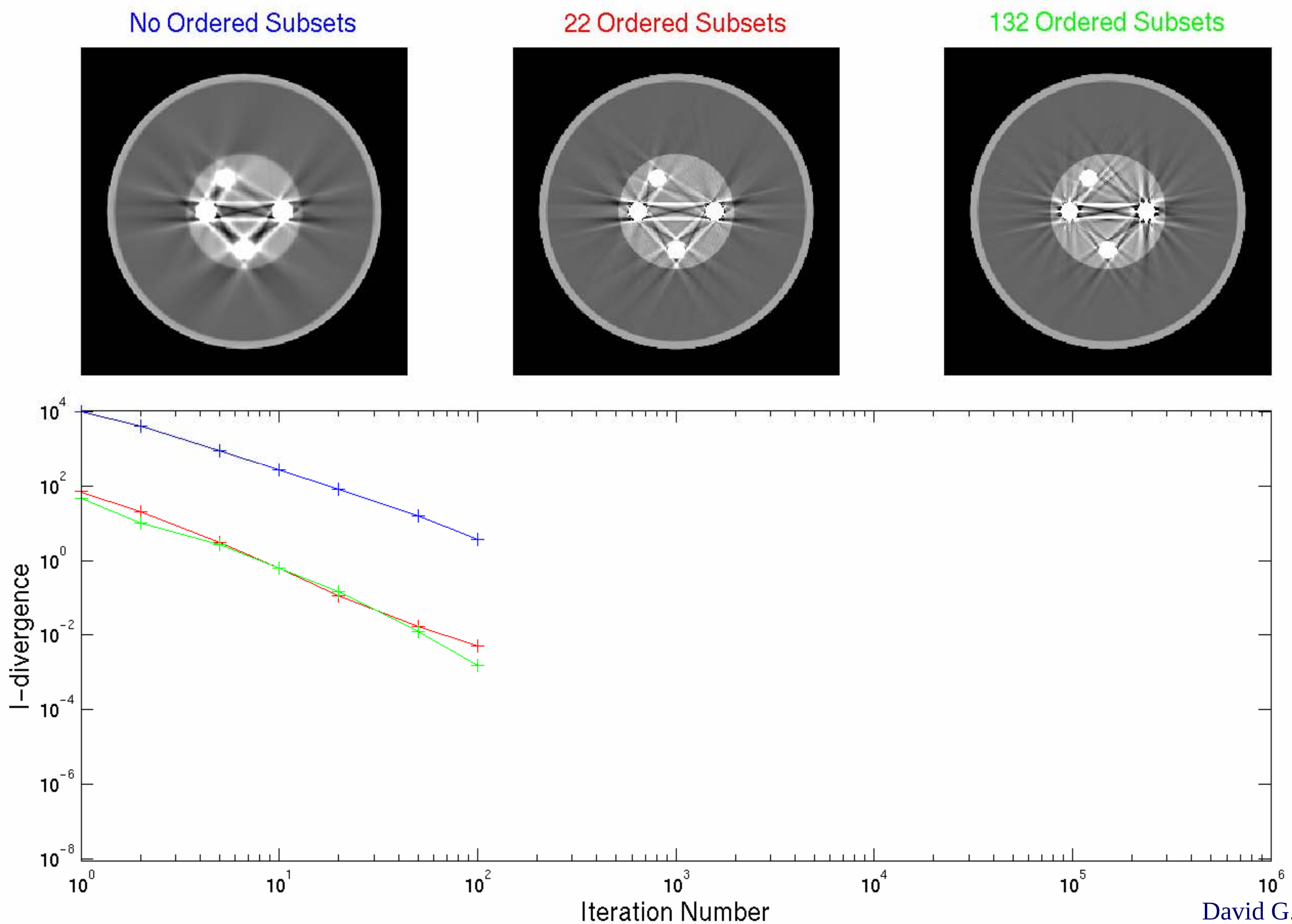

David G. Politte
October 31, 2002

Mini CT, AM Iteration 0000200

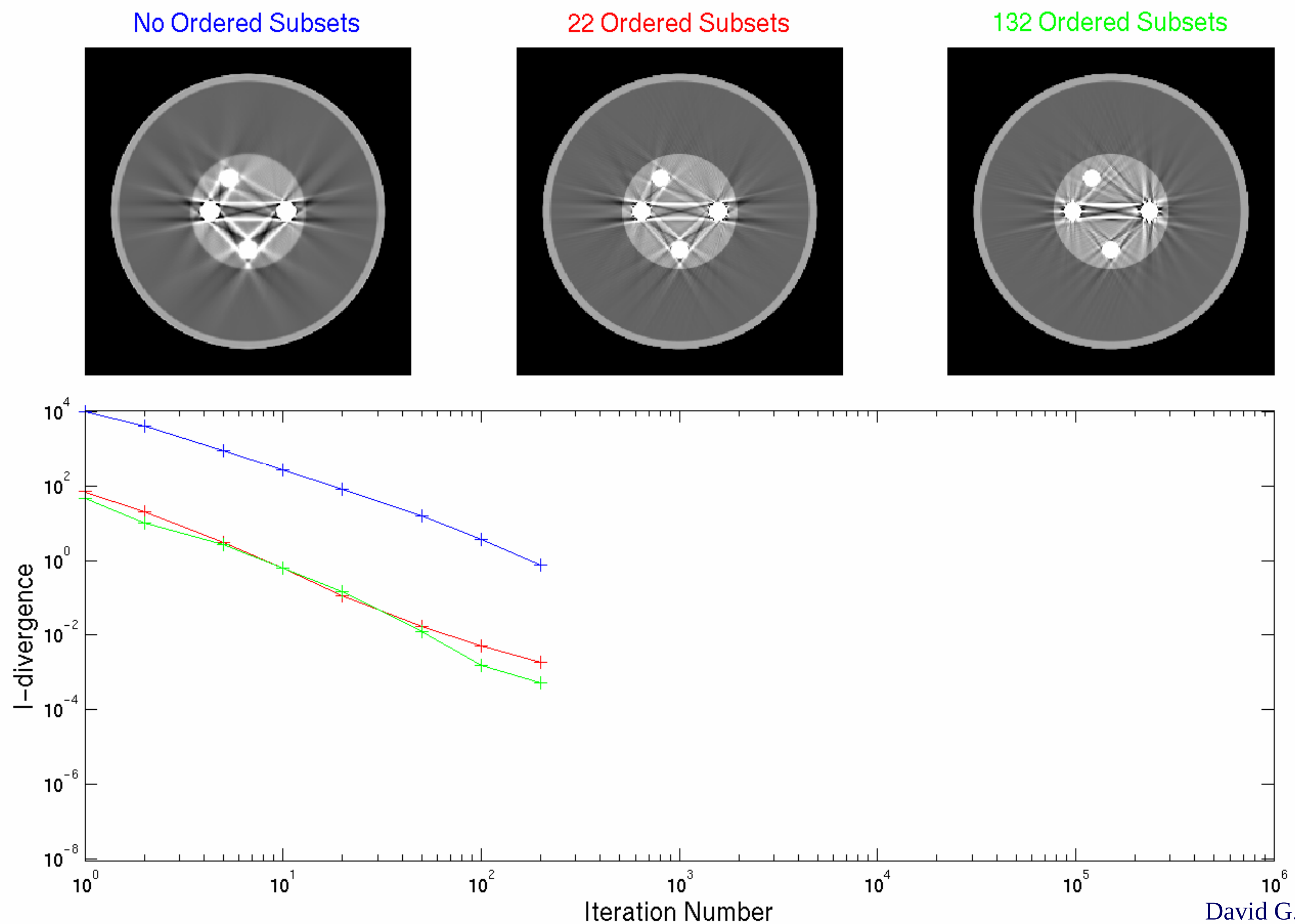

David G. Politte
October 31, 2002

Mini CT, AM Iteration 0000500

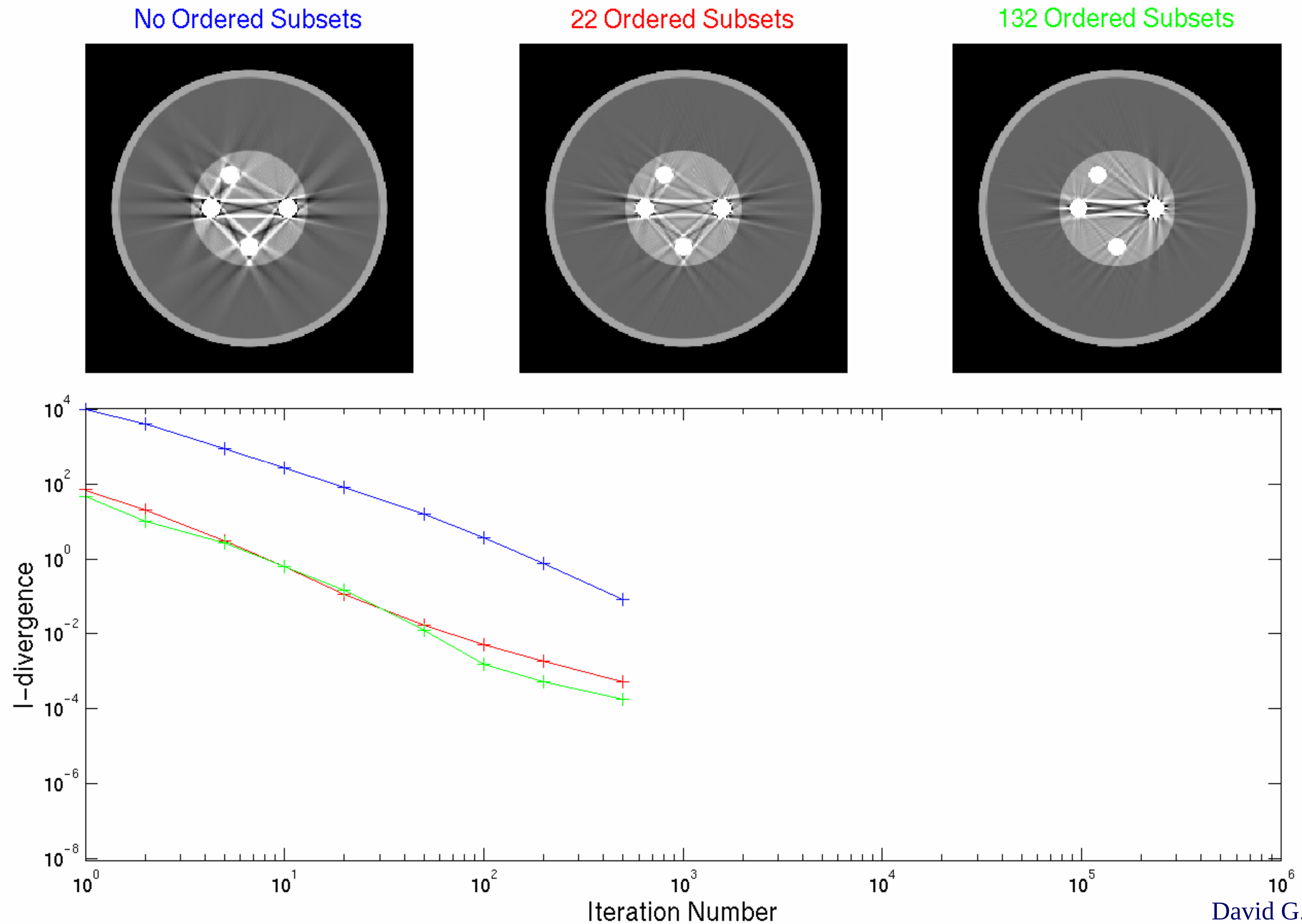

David G. Politte
October 31, 2002

Mini CT, AM Iteration 0001000

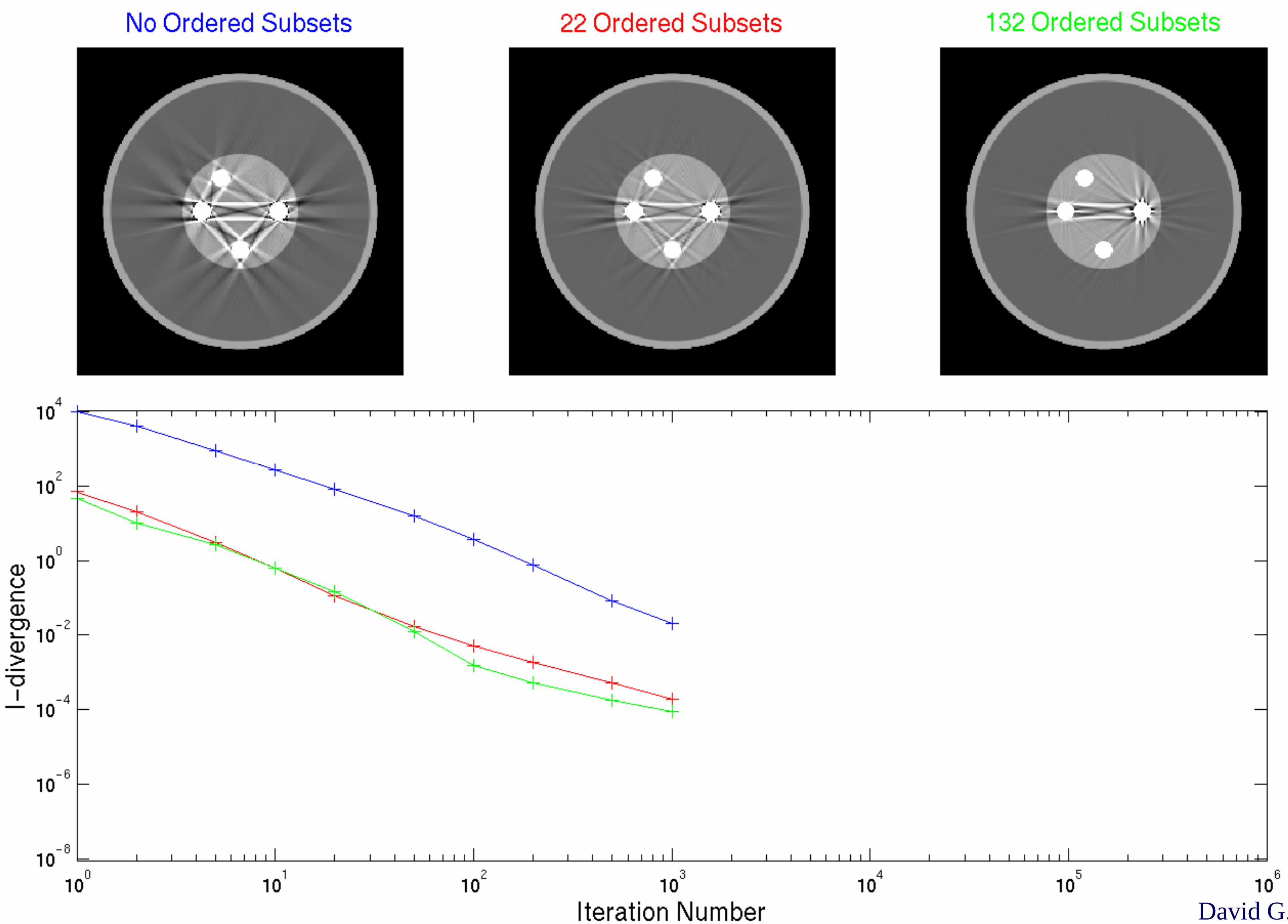

David G. Politte
October 31, 2002

Mini CT, AM Iteration 0002000

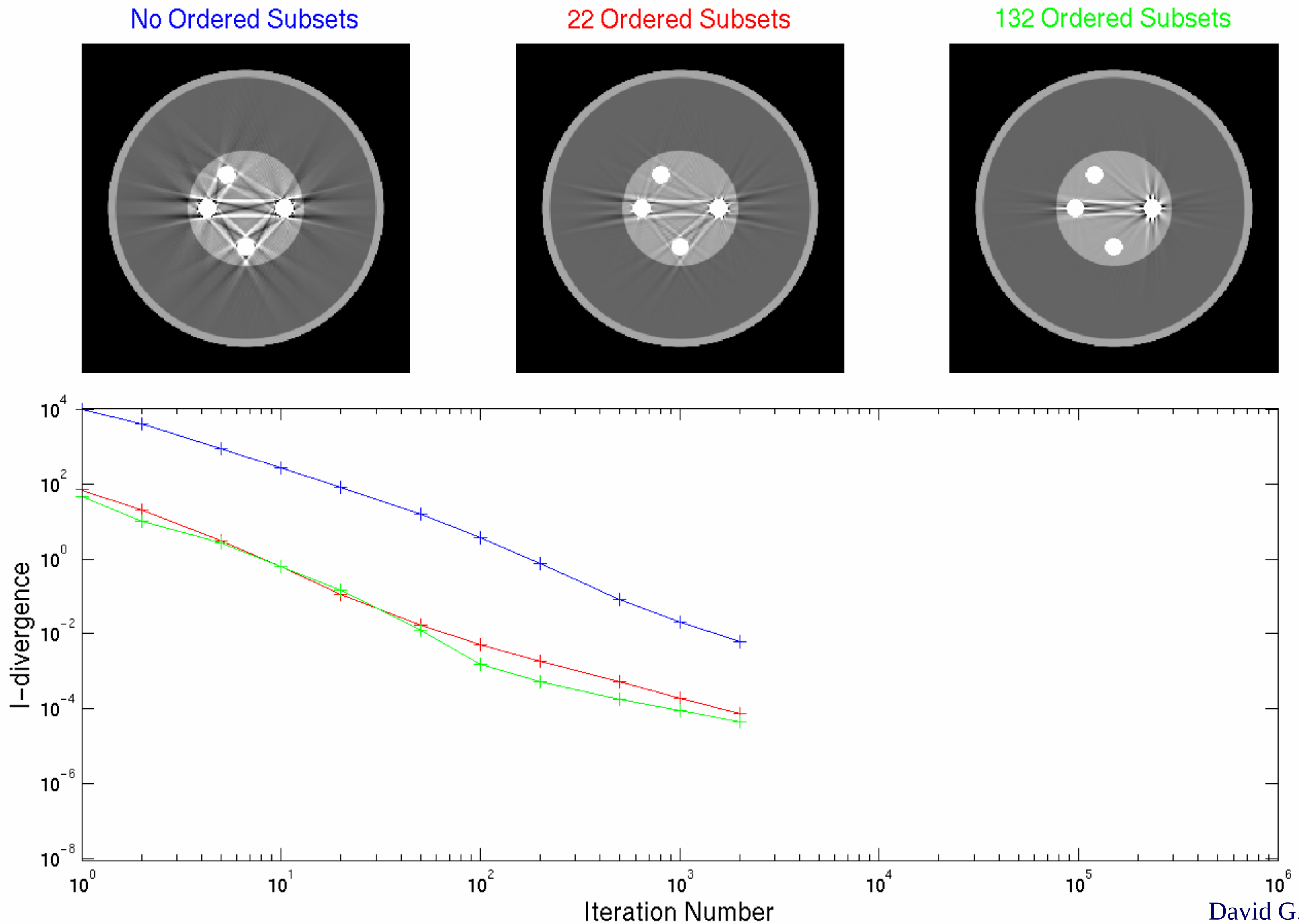

David G. Politte
October 31, 2002

Mini CT, AM Iteration 0005000

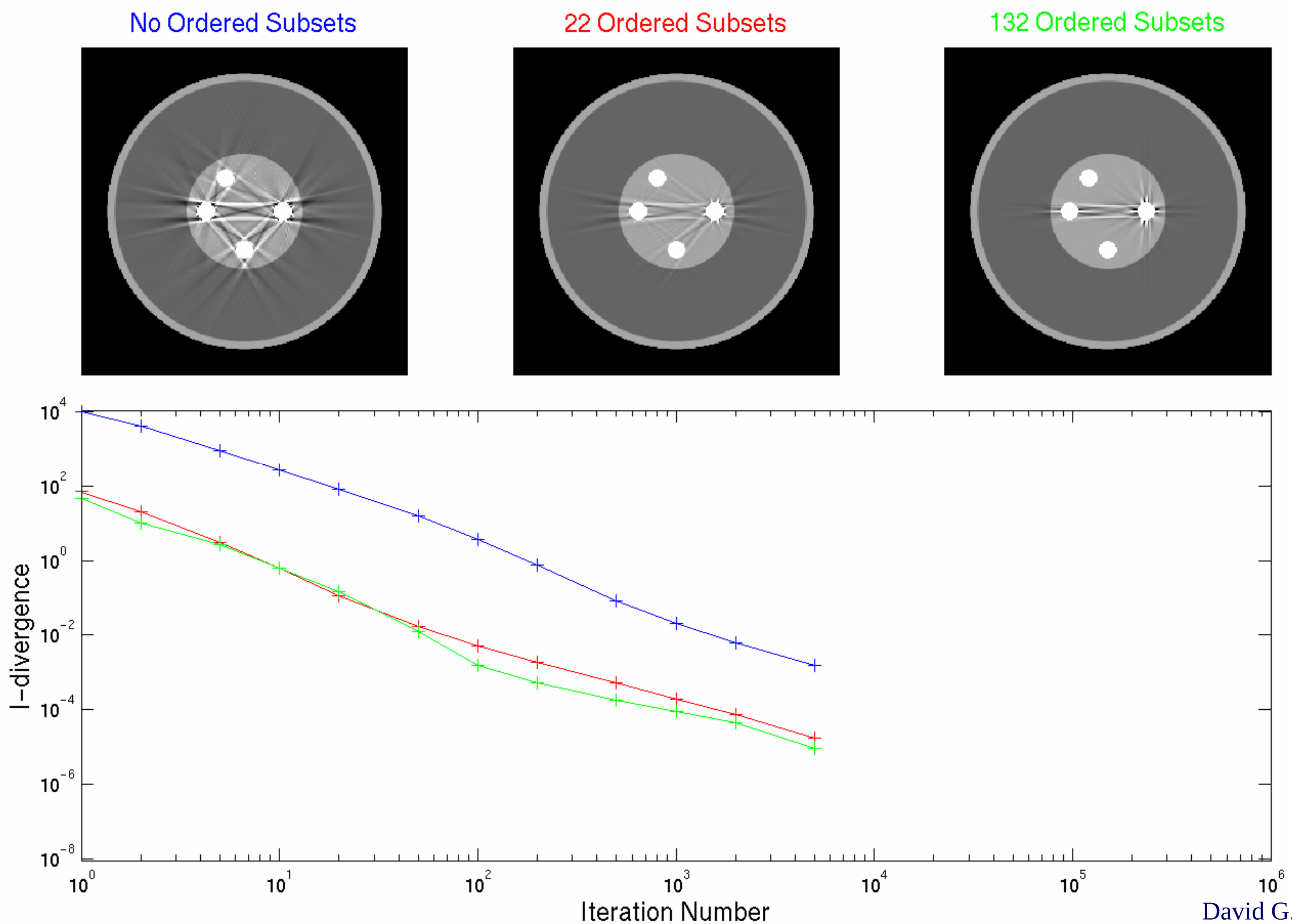

David G. Politte
October 31, 2002

Mini CT, AM Iteration 0010000

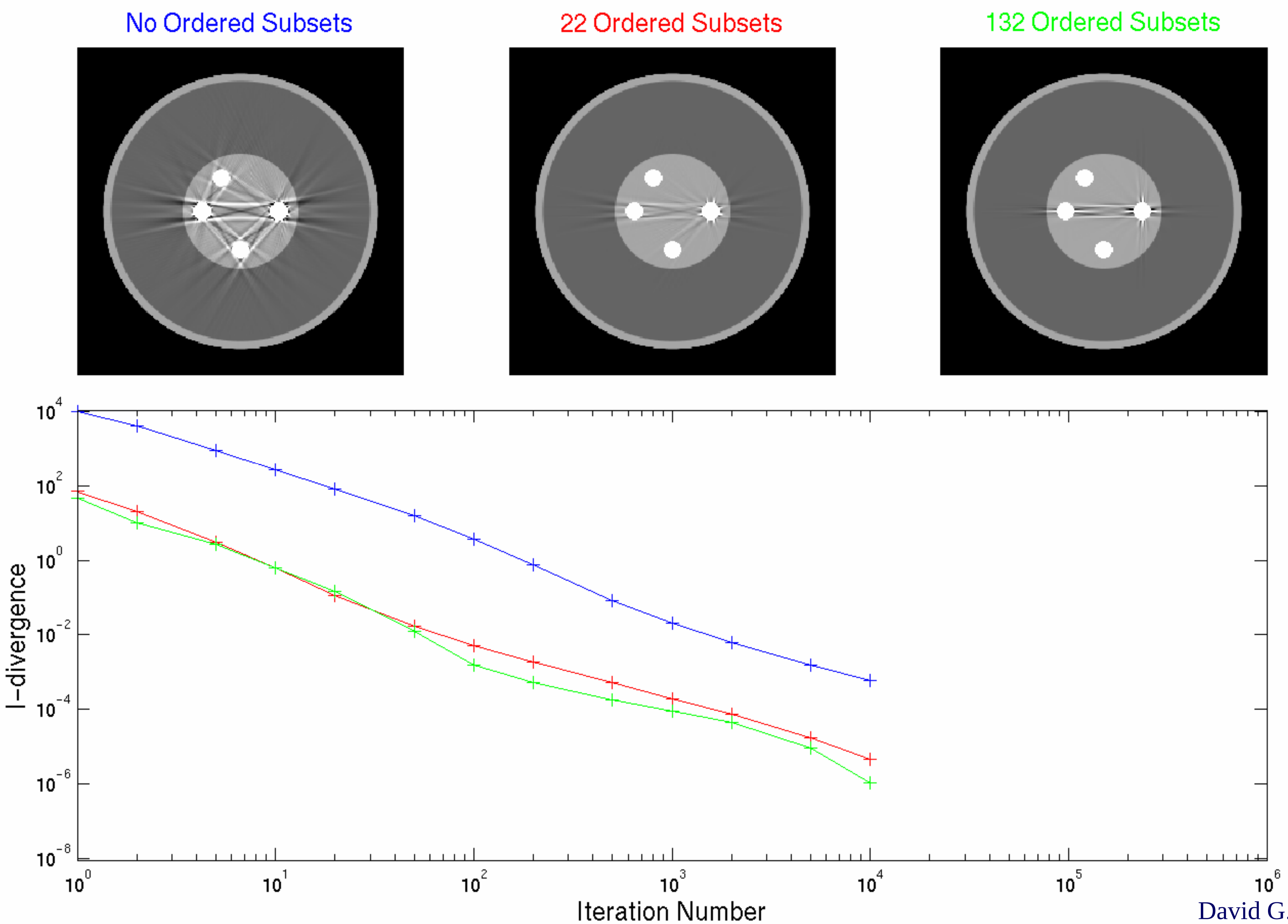

David G. Politte
October 31, 2002

Mini CT, AM Iteration 0020000

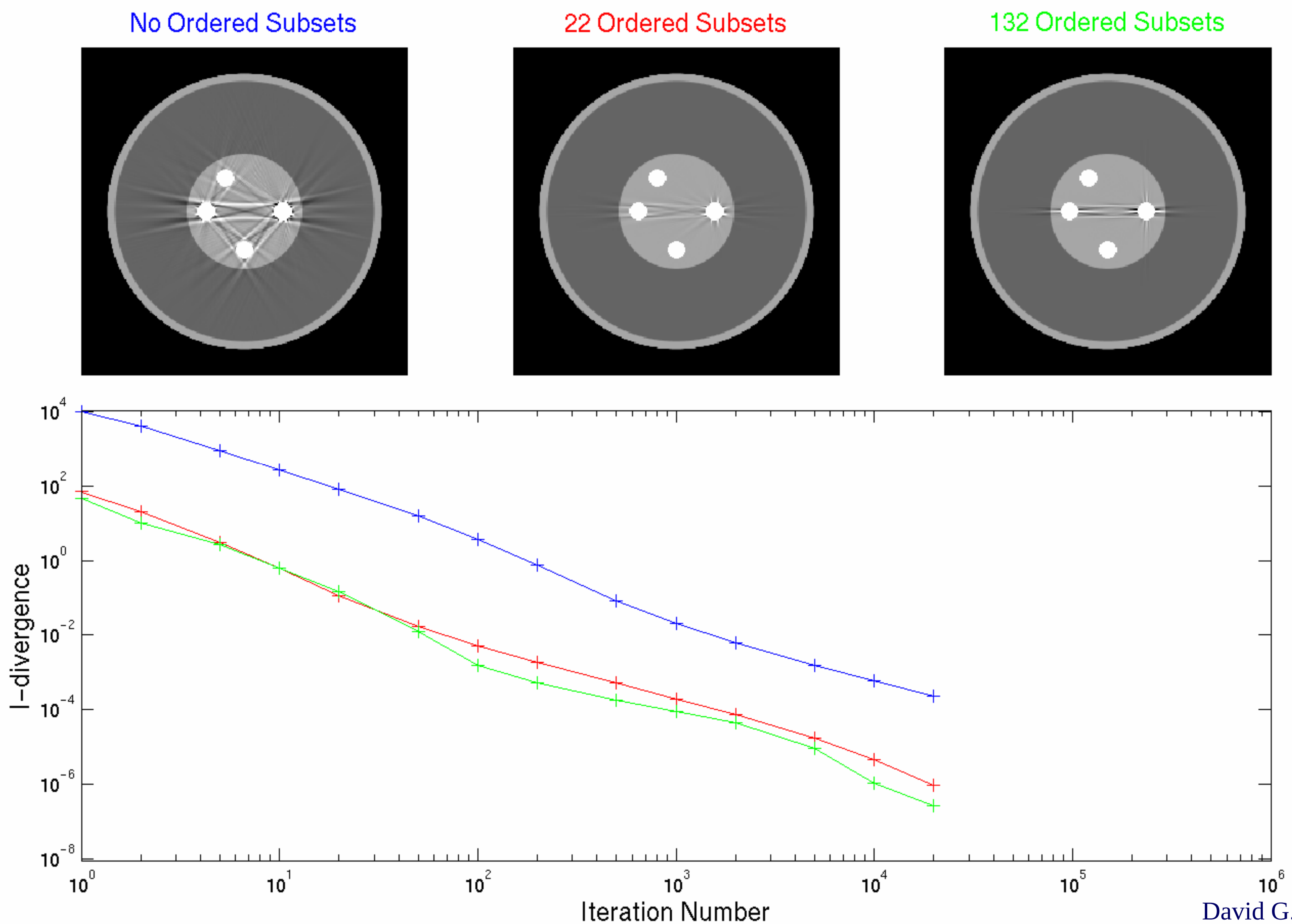

David G. Politte
October 31, 2002

Mini CT, AM Iteration 0050000

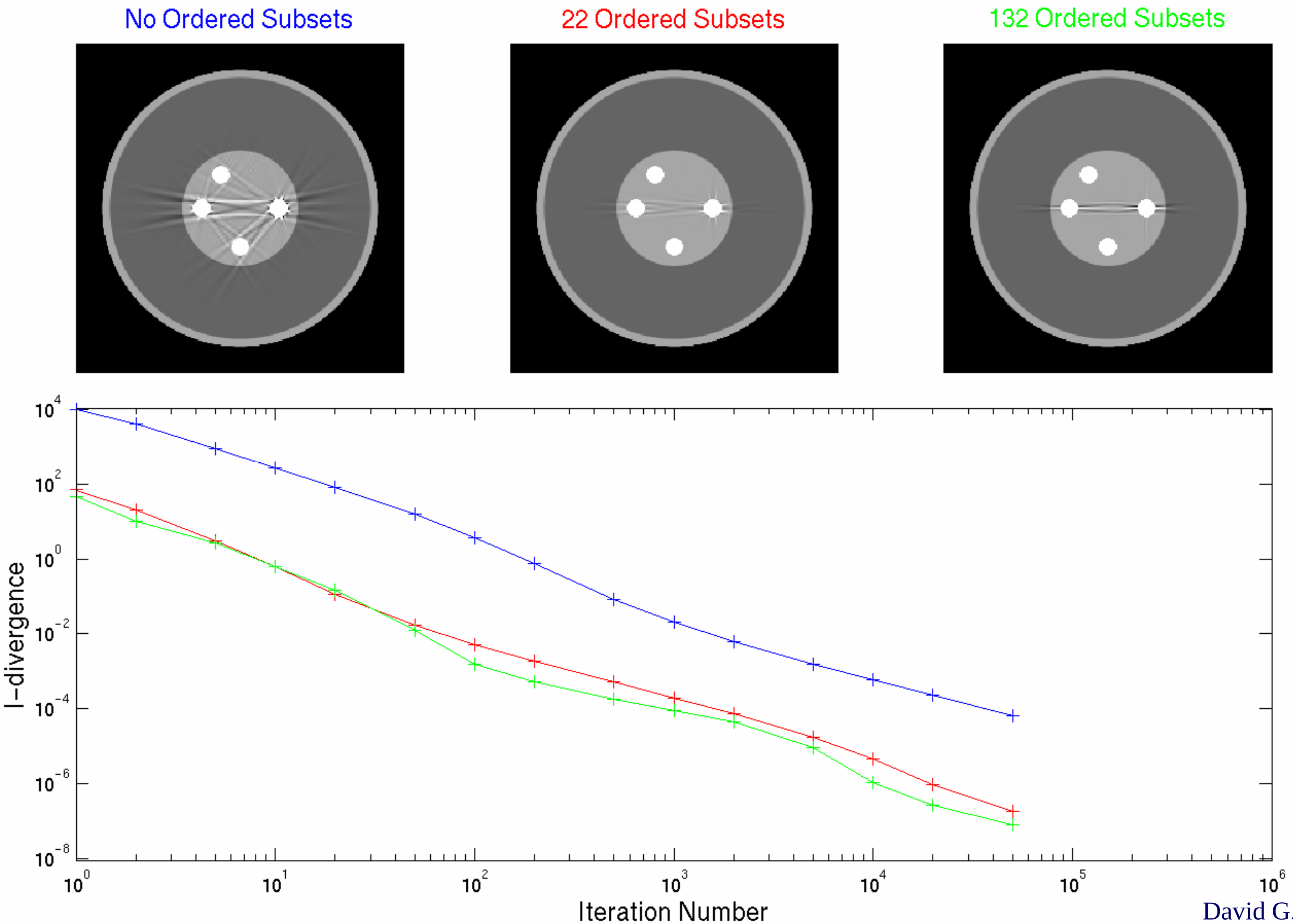

David G. Politte
October 31, 2002

Mini CT, AM Iteration 0100000

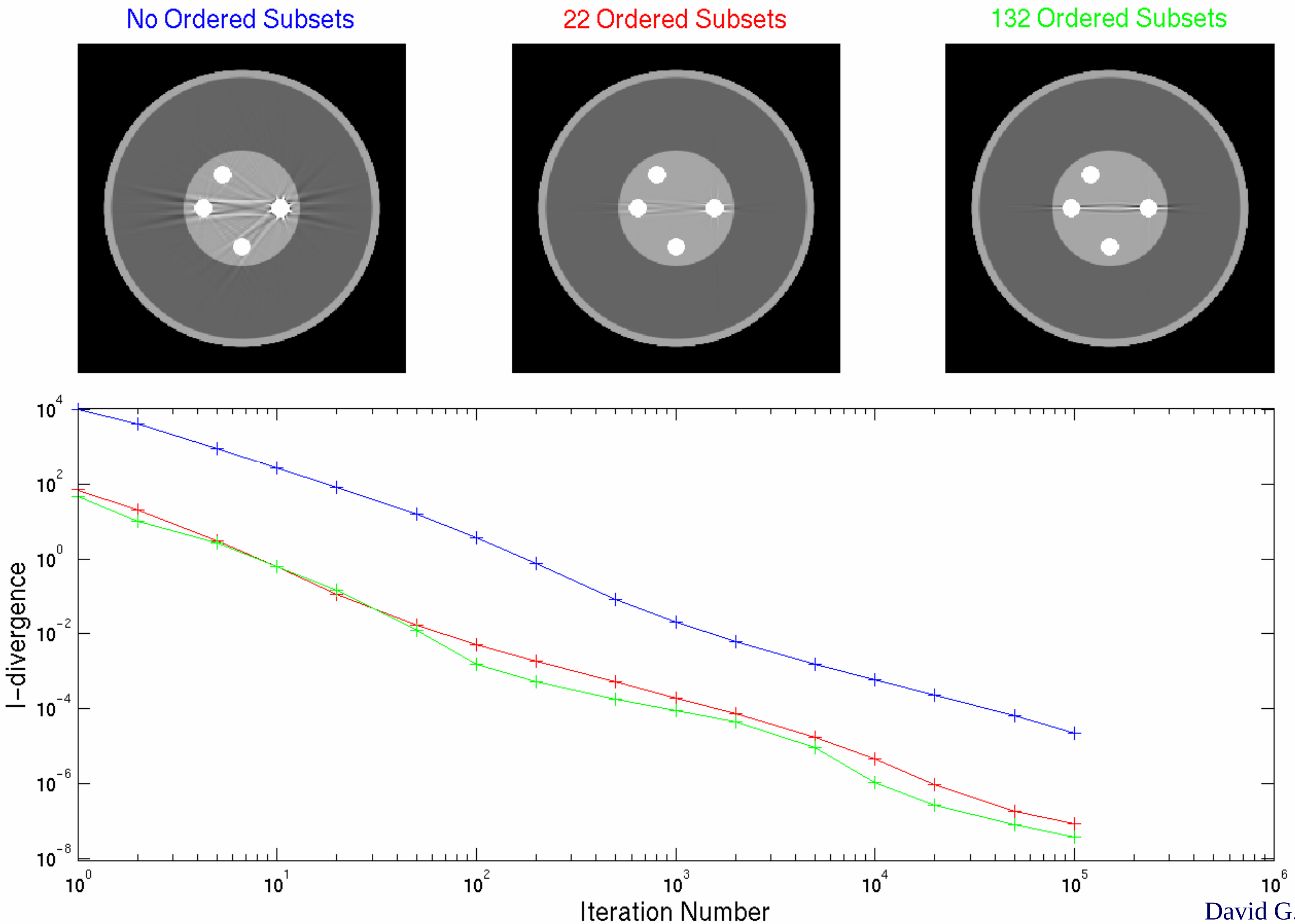

David G. Politte
October 31, 2002

Mini CT, AM Iteration 0200000

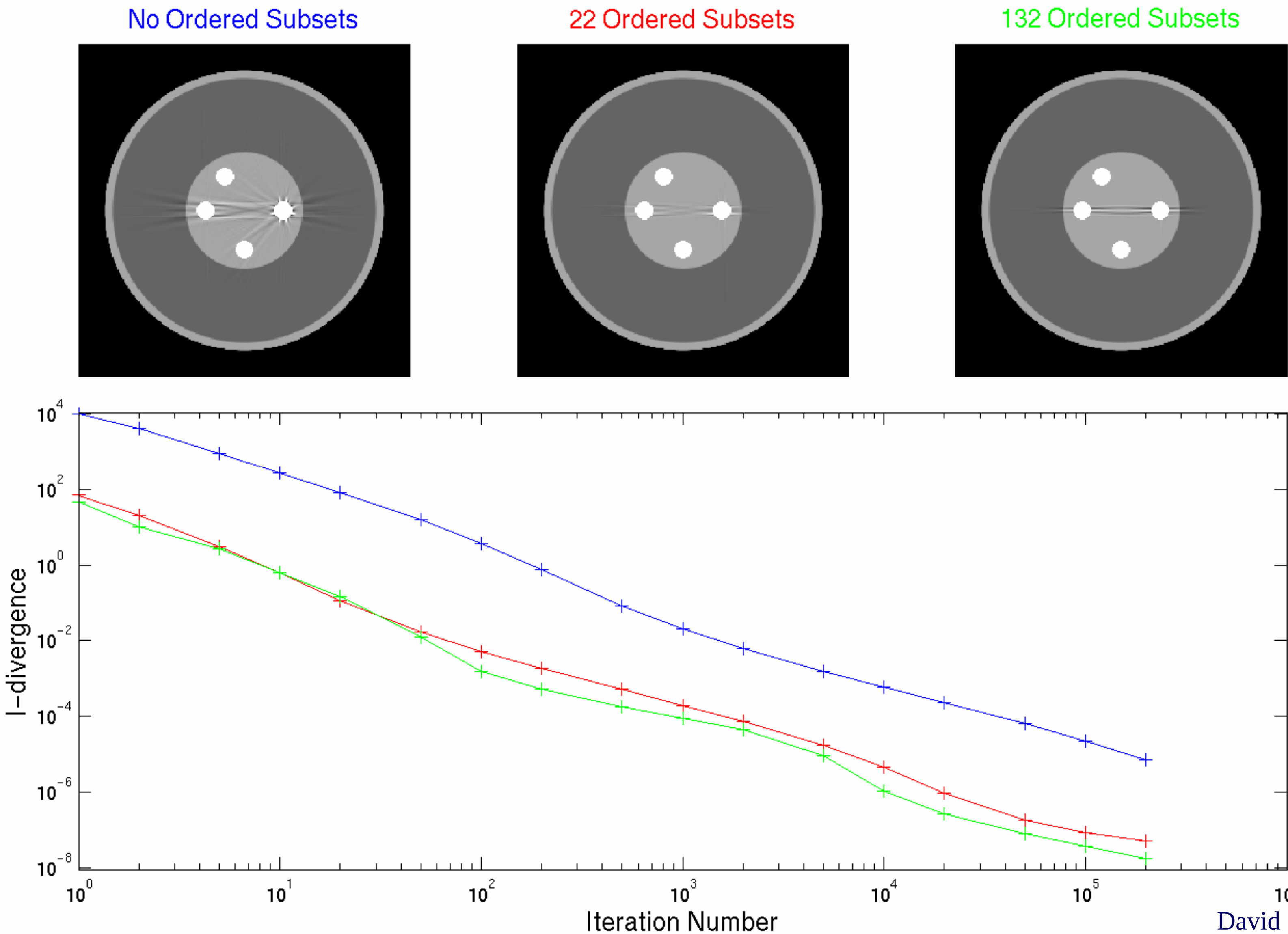

David G. Politte
October 31, 2002

Mini CT, AM Iteration 0500000

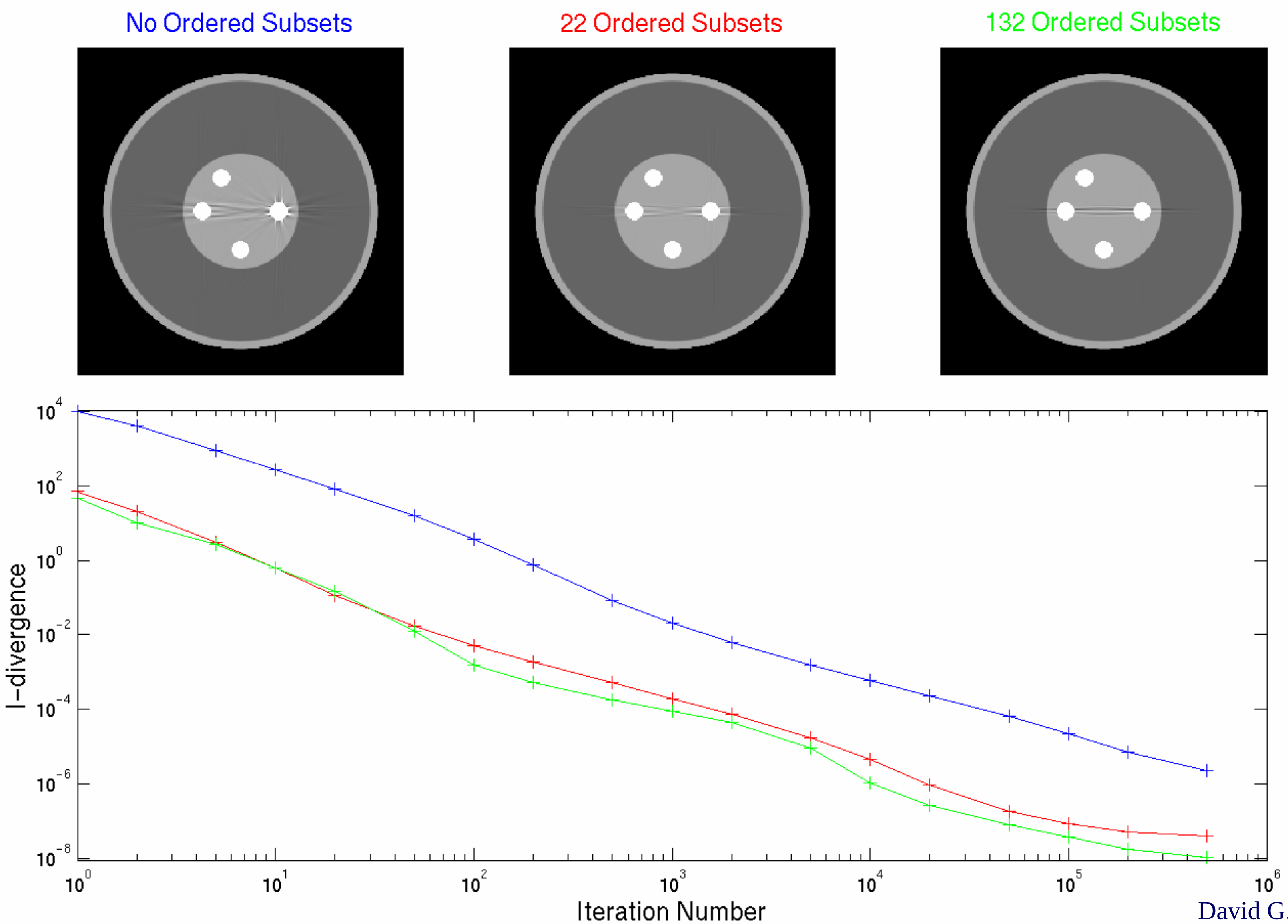

David G. Politte
October 31, 2002

Mini CT, AM Iteration 1000000

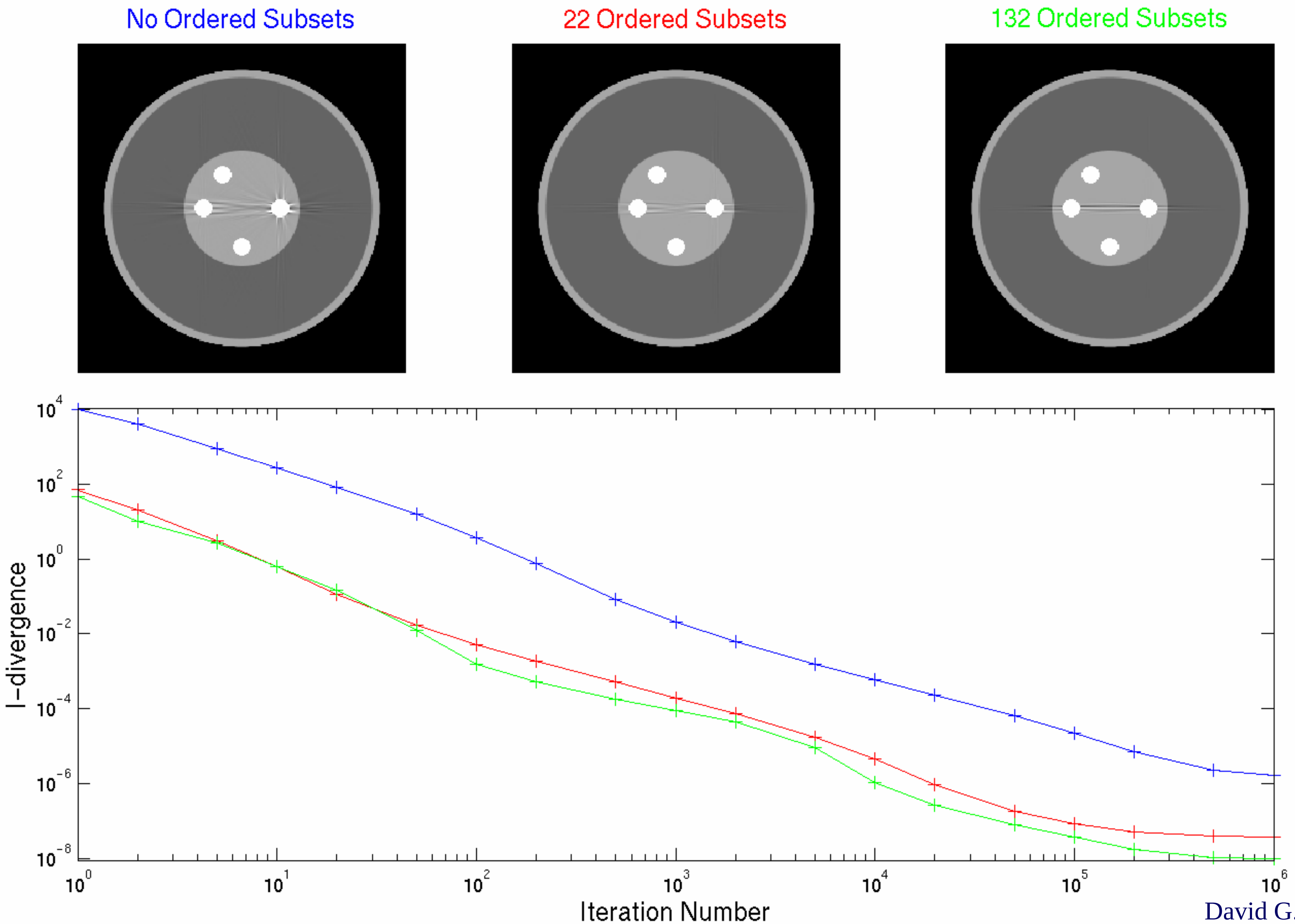

David G. Politte
October 31, 2002

Iterative Algorithm with Known Applicator Pose

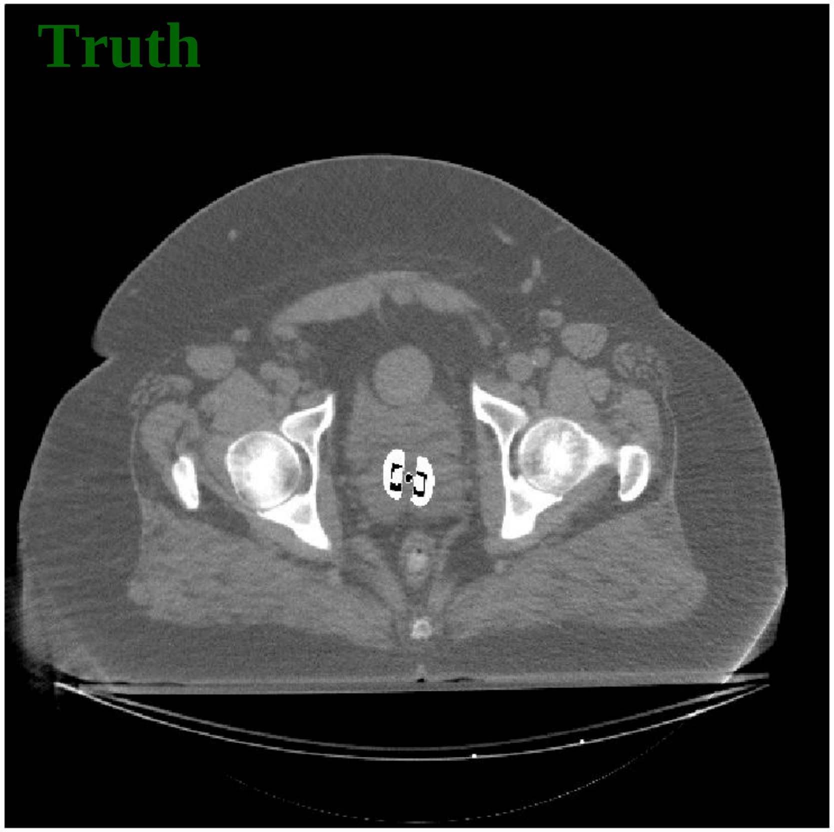

OCCT Iterations

OCCT

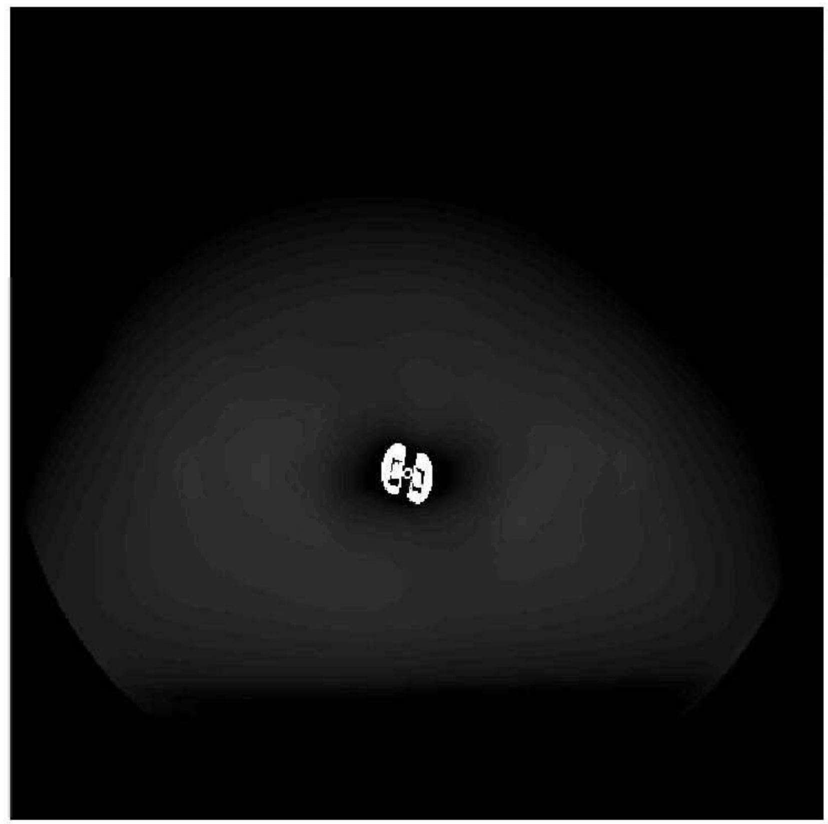

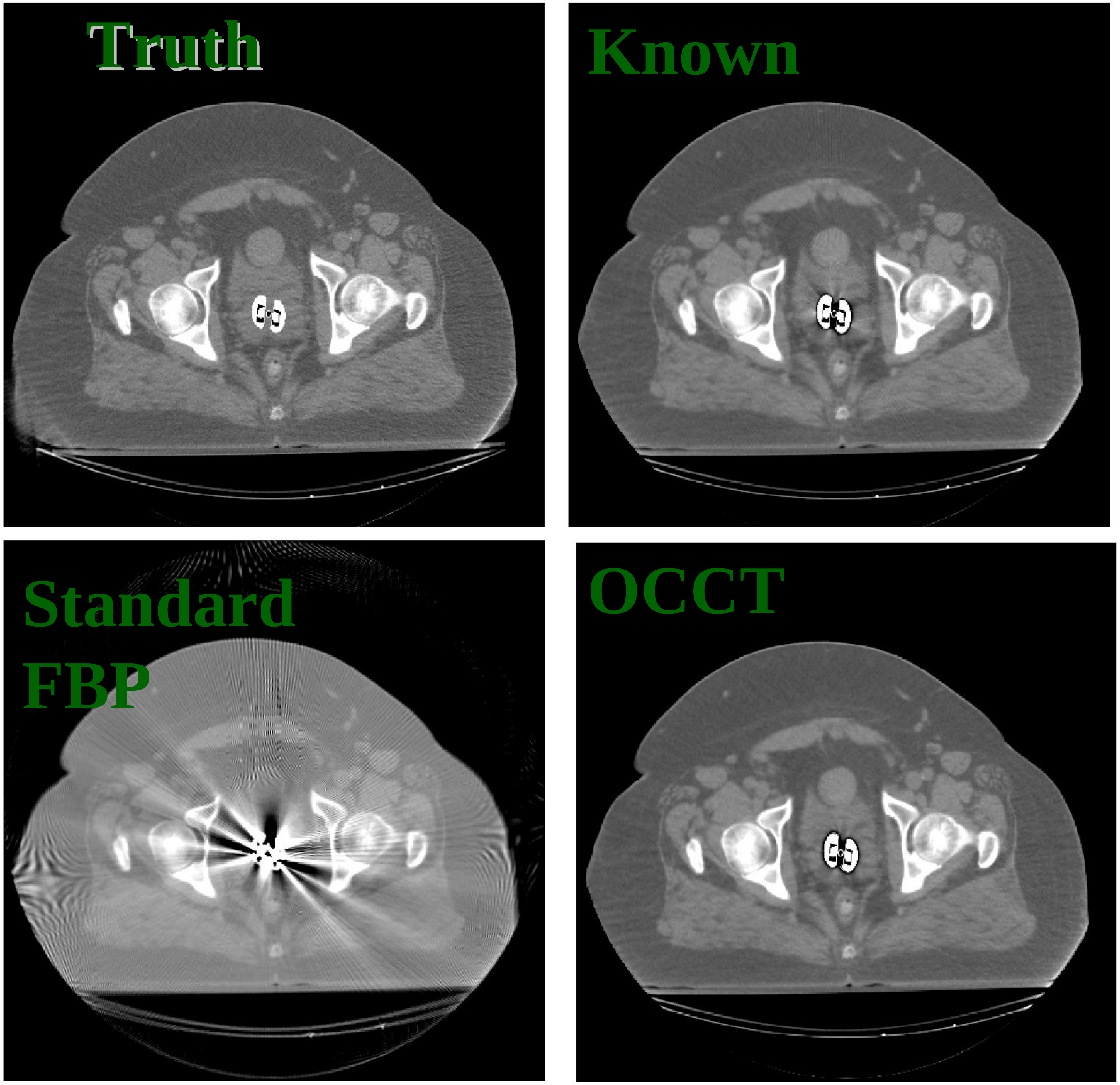
Truth
Known
Standard FBP
OCCT

Magnified views around brachytherapy applicator

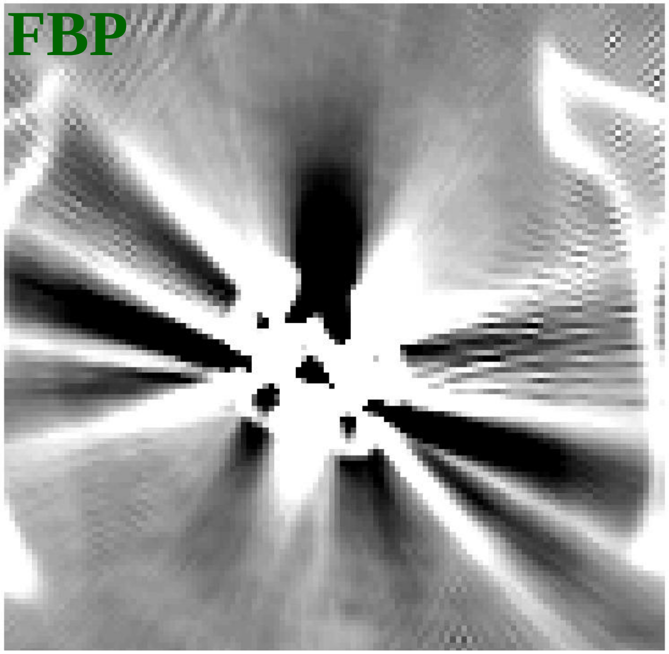

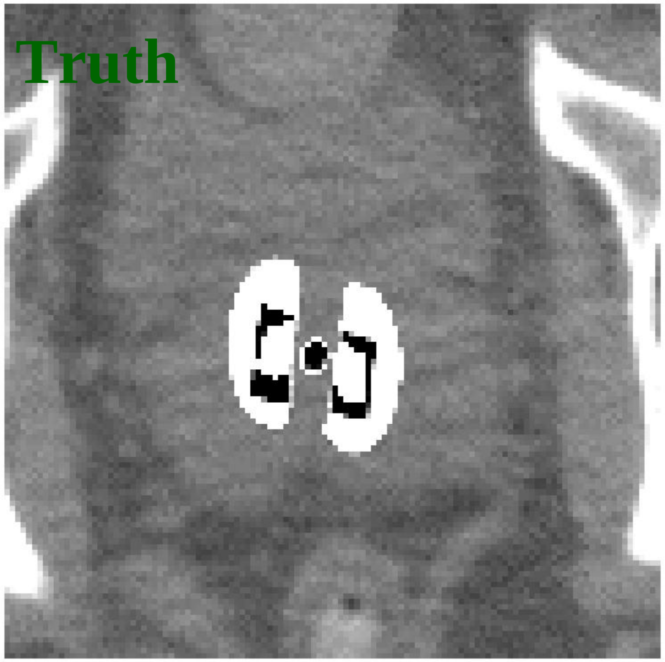

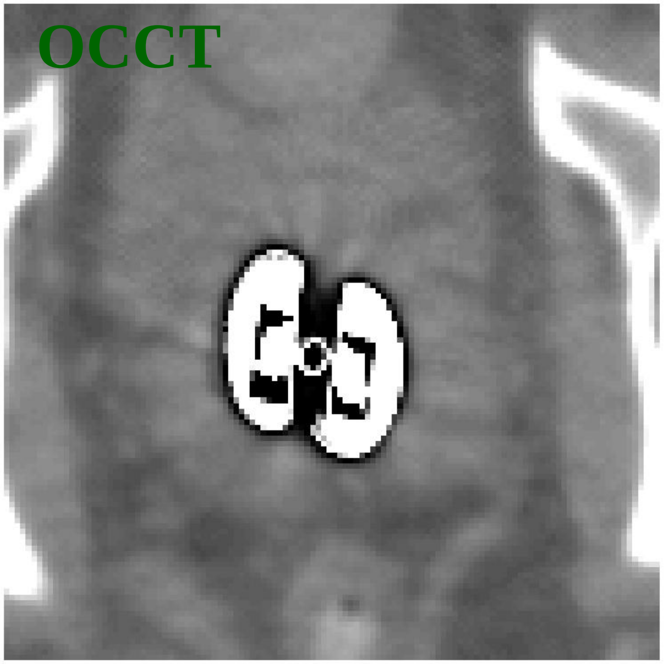

Additional Algorithm/Detector Model Development

- Regularization
- Energy integrating detectors $\int E dN(y,E)$
- Finite detector size, better source model
- Finite pixel, voxel size
- Average integral or average exponential (arithmetic vs. geometric average)
- Partial volume effects
- Motion
- Scattering
- Limited angle tomography
- Region of interest
- Scanner implementations: beam hardening correction, sampling, etc.

Real Data Experiments & Considerations of Region-of-Interest Tomography

LOW DENSITY ROD PHANTOM

(DLS, R. Murphy, 06/25/03)

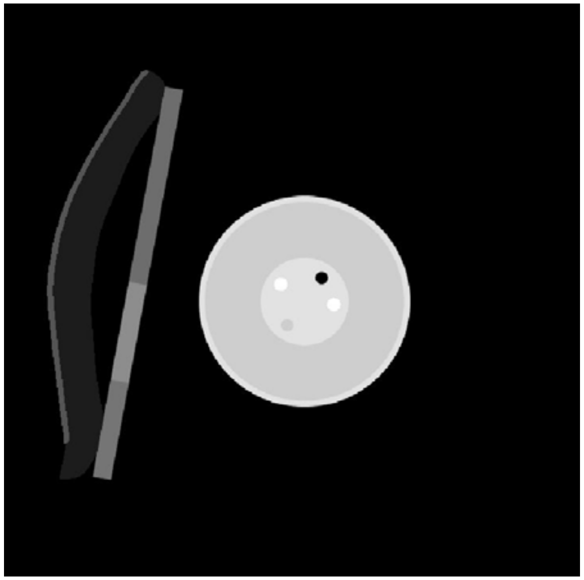

Rods are:
Air
Teflon
Water
Aluminum

Board Inside FOV

Synthetic

AM

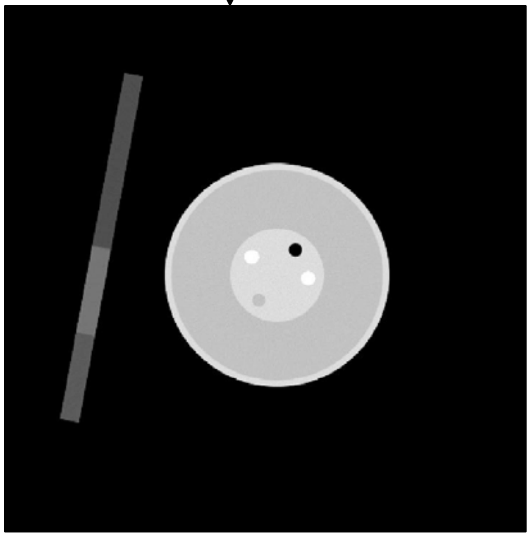

1000 (22)

Board Outside FOV

Synthetic

AM

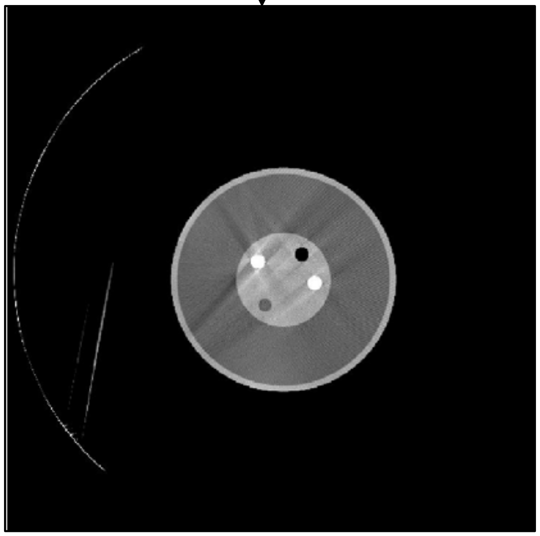

1000 (22)

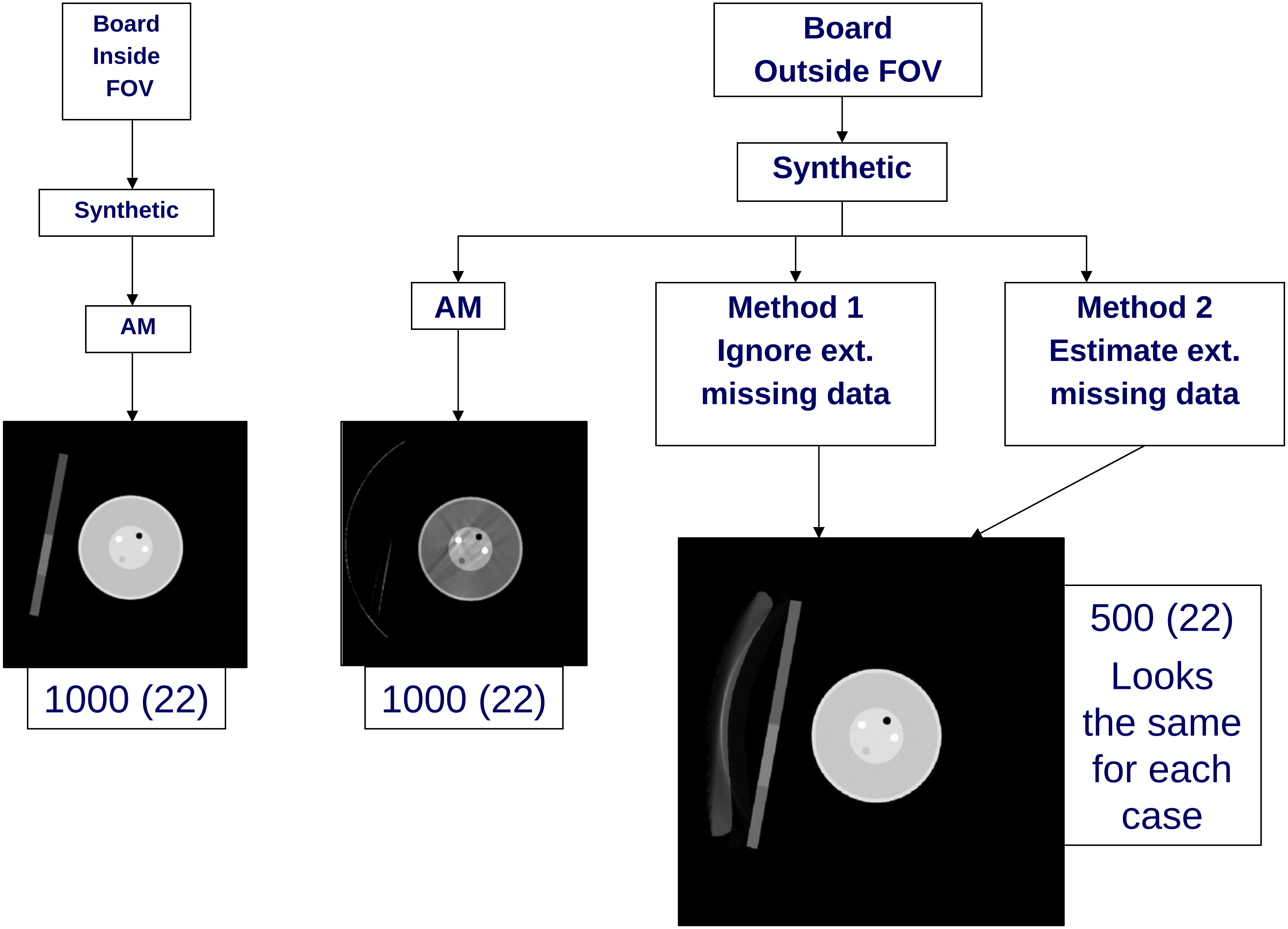
Board Inside FOV
Synthetic
AM
1000 (22)
Board Outside FOV
Synthetic
AM
1000 (22)
Method 1 Ignore ext. missing data
Method 2 Estimate ext. missing data
500 (22)
Looks the same for each case

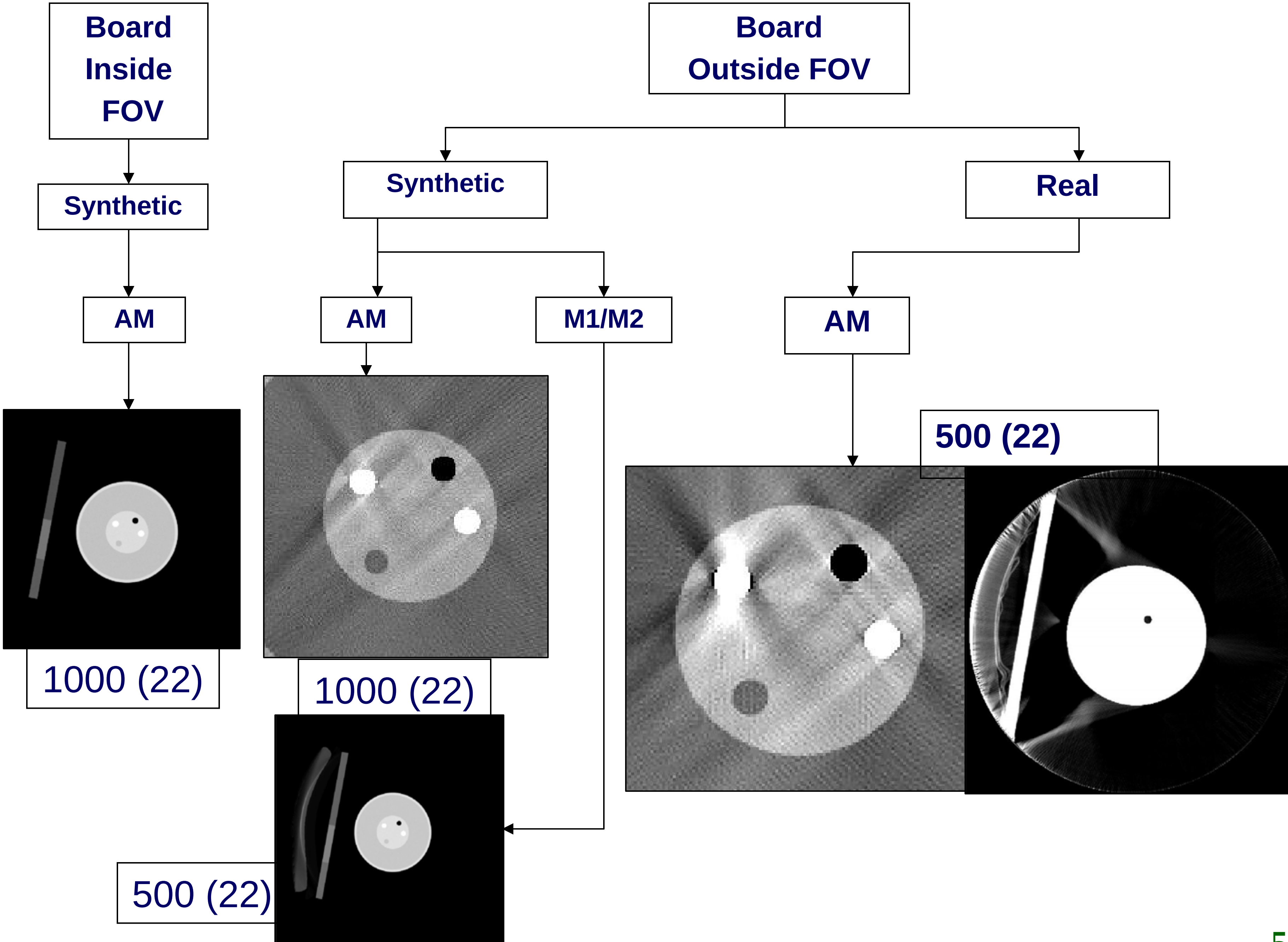
Board Inside FOV
Synthetic
AM
1000 (22)
Board Outside FOV
Synthetic
AM
1000 (22)
M1/M2
500 (22)
Real
AM
500 (22)

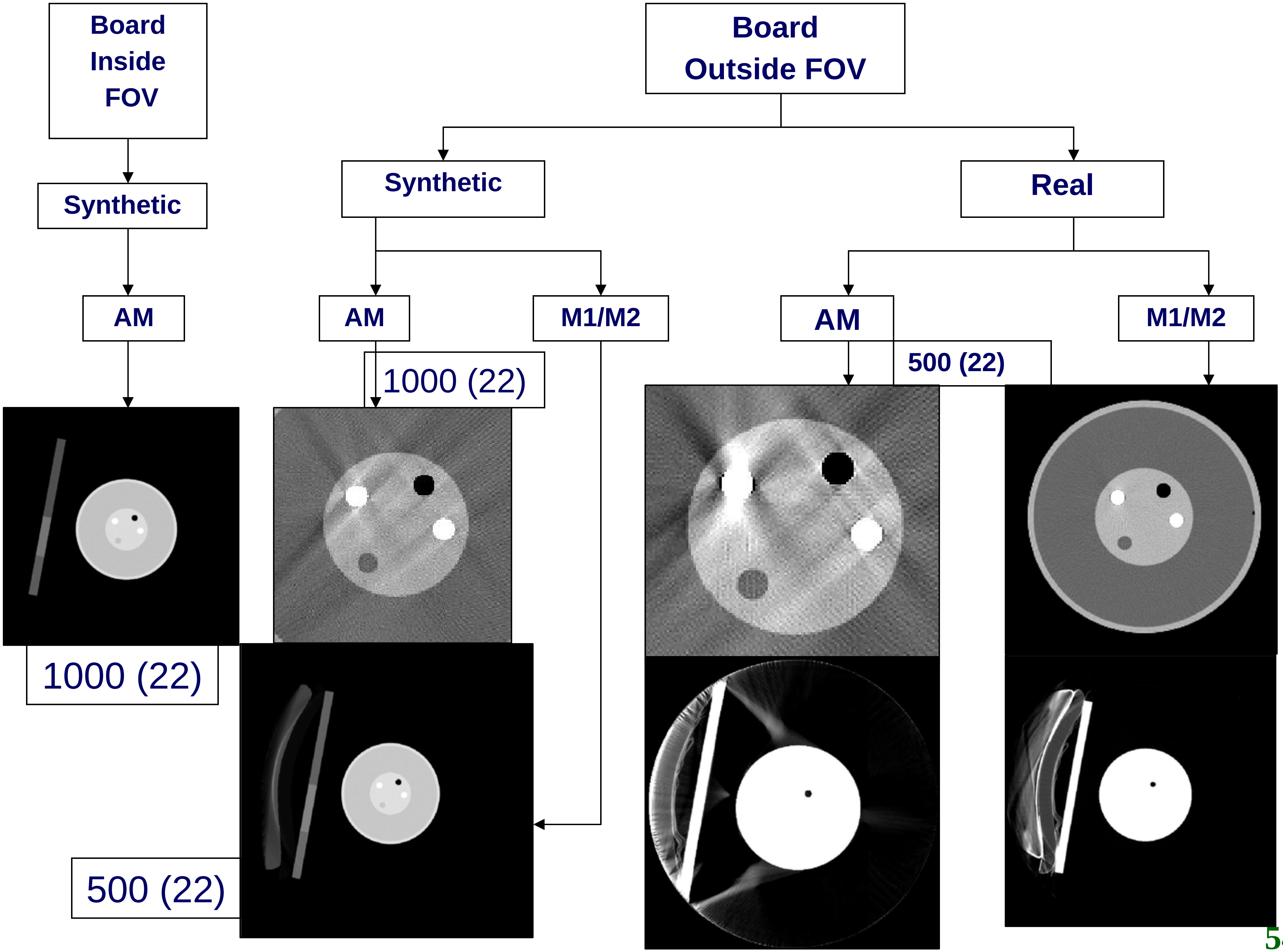
Board Inside FOV
Synthetic
AM
1000 (22)
Board Outside FOV
Synthetic
AM
1000 (22)
M1/M2
500 (22)
Real
AM
500 (22)
M1/M2

Real data reconstruction

Replace rod projection via masking

50 it (22 OS) | 500 it (22 OS) | 200 it (22 OS)

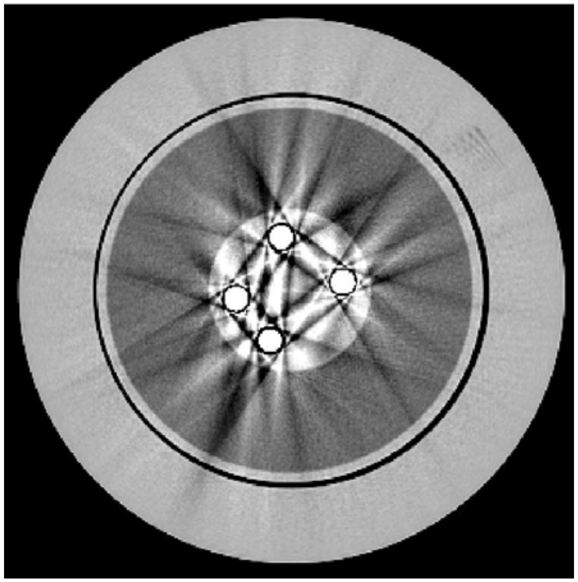

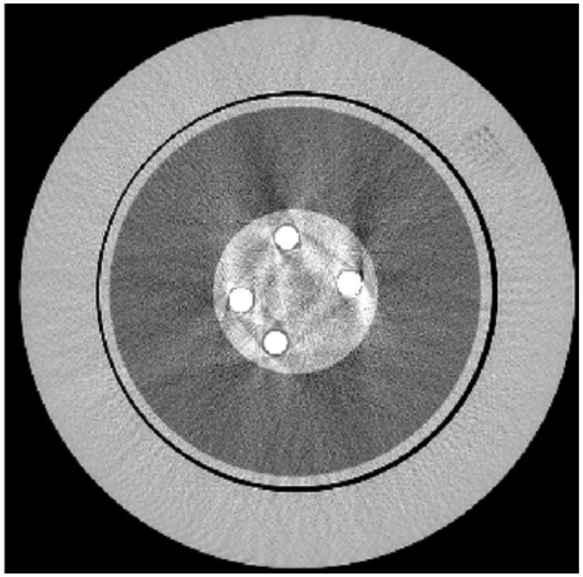

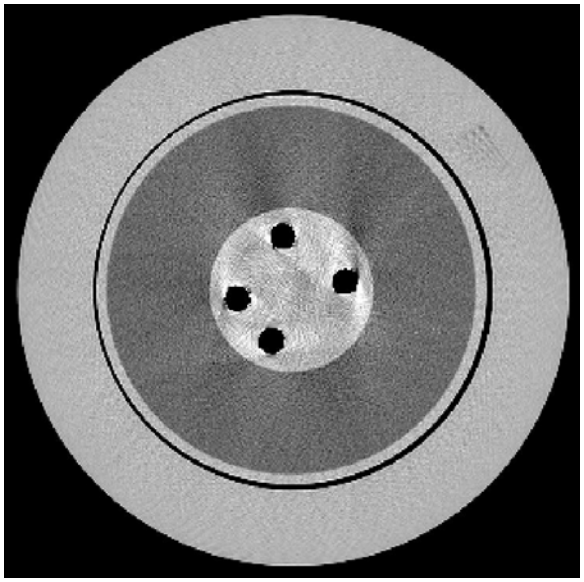

Method 2—(replace with q(y))

Method 1—(replace with 0)

I.C. just rods

I.C. water + rods

Data reconstruction w/ pose search

80 it (22 OS) | 200 it (22 OS) | 200 it (22 OS)

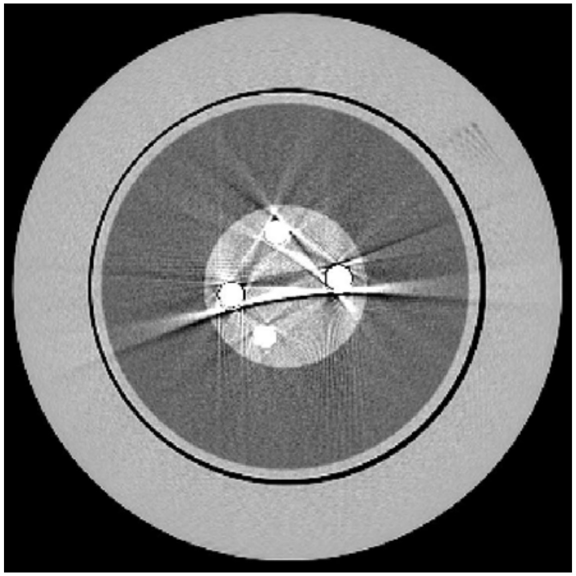
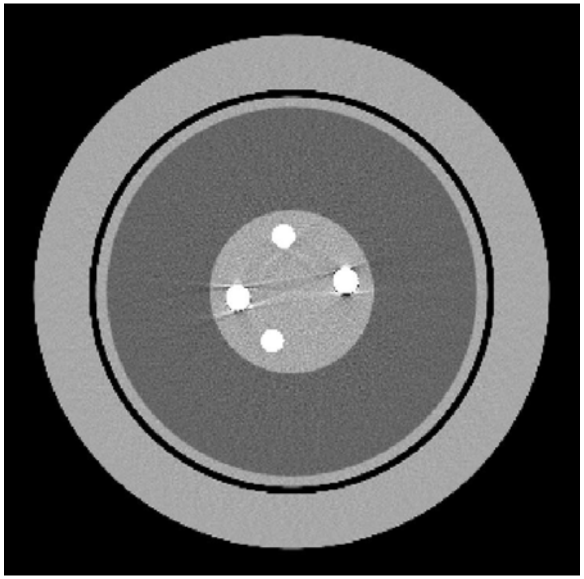
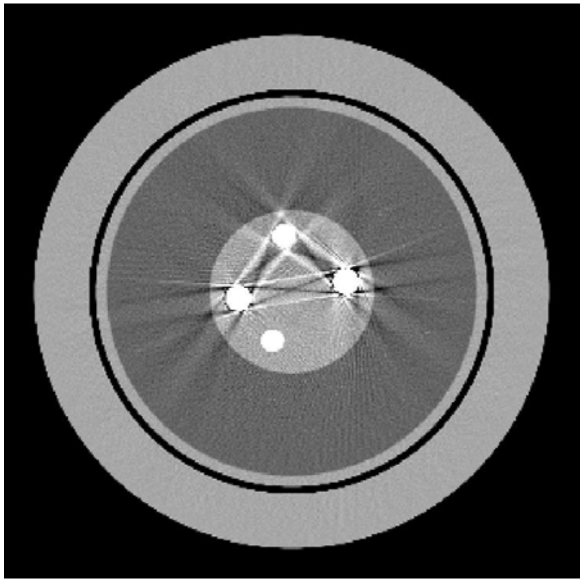

Precorrected real data

Synthetic data

Uses correct attenuation values

Uses incorrect attenuation values

AM performance with multi-component tissue model

Data means:

$$g(y)=\sum_E I_0(y,E)\exp\left[-\sum_X h(y|x)\mu(x,E)\right]+\beta(y)$$

$$\mu(\boldsymbol{x},\boldsymbol{E})=\sum_{\boldsymbol{i}=1}^{\boldsymbol{I}}\mu_{\boldsymbol{i}}(\boldsymbol{E})\boldsymbol{c}_{\boldsymbol{i}}(\boldsymbol{x})$$

$\mu_i(\mathbf{E})$ – linear attenuation coefficient [mm^{-1}]

$c_i(x)$ – specific gravity [unitless]

AM update step: $$\hat{\boldsymbol{c}}_{\boldsymbol{i}}^{(\boldsymbol{k}+1)}=\hat{\boldsymbol{c}}_{\boldsymbol{i}}^{(\boldsymbol{k}+1)}(\boldsymbol{x})-\frac{1}{\boldsymbol{Z}_{\boldsymbol{i}}(\boldsymbol{x})}\ln\left(\frac{\tilde{\boldsymbol{b}}_{\boldsymbol{i}}^{(\boldsymbol{k})}(\boldsymbol{x})}{\hat{\boldsymbol{b}}_{\boldsymbol{i}}^{(\boldsymbol{k})}(\boldsymbol{x})}\right)$$

Multi-component experiment setup

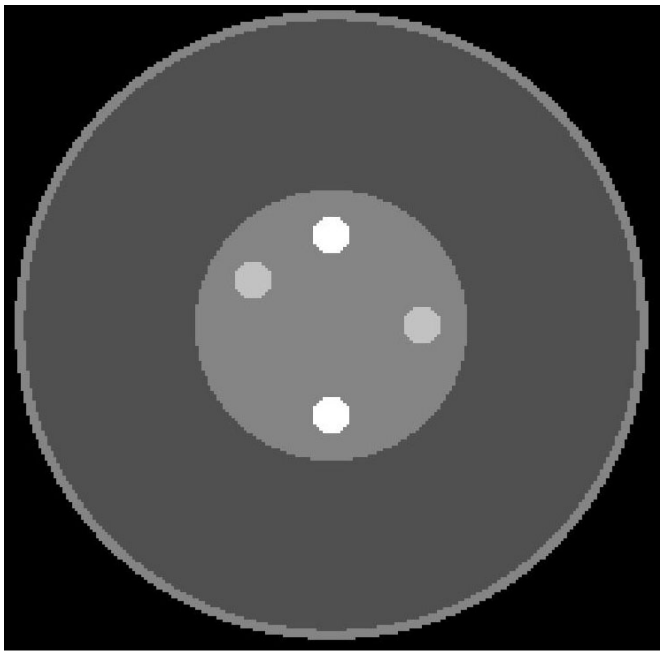

Substance	True $c_1(x)$	True $c_2(x)$
Water	0.9036	0.1357
Lucite	1.14	0.0583
Muscle	0.9399	0.1390
Ethanol	0.7999	0.0337
Teflon	1.4194	0.4878
X	0.0300	2.8613

Inserts (Muscle, Ethanol, Teflon, X)

$\mu_1(E)$ – Styrene

$\mu_2(E)$ – Ca Chloride

Multi-component experiment setup

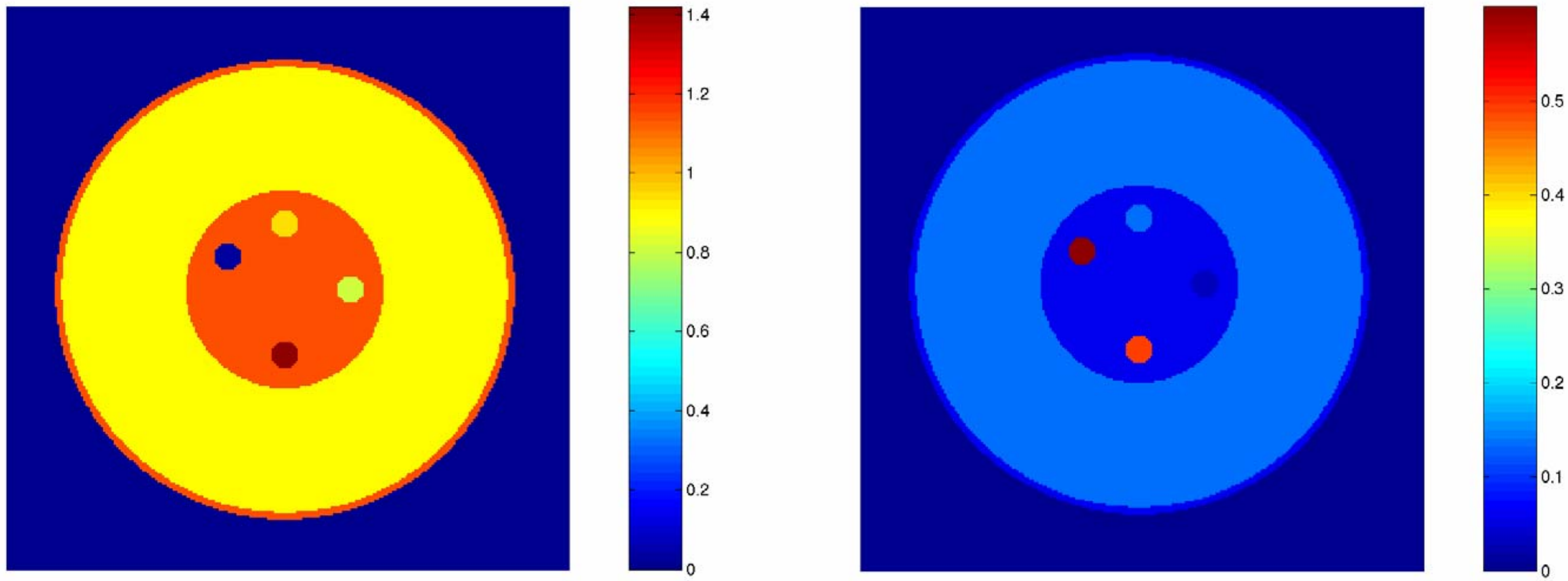

True $c_1(x)$ True $c_2(x)$

$$g(y) = \sum_E I_0(y,E)\exp\left[-\sum_X h(y|x)\mu(x,E)\right] + \beta(y)$$

AM performance with multi-component tissue model

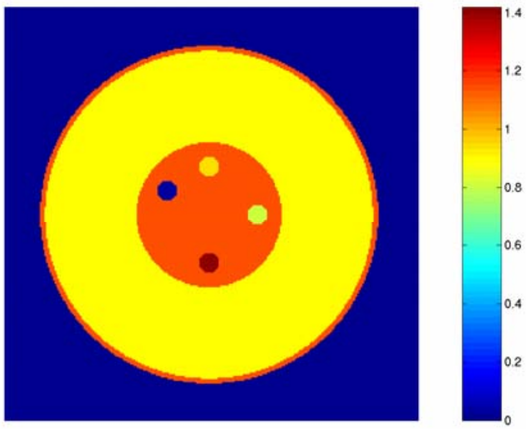

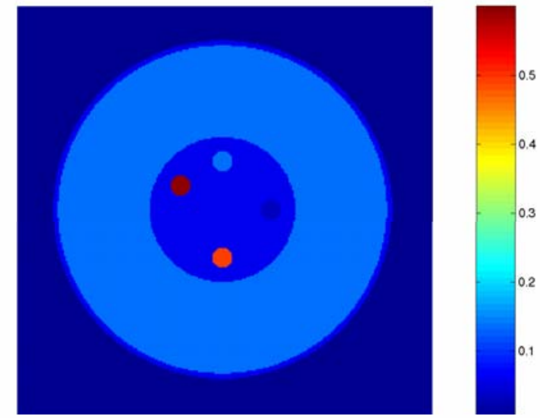

AM reconstructed images

100 iterations (22OS)

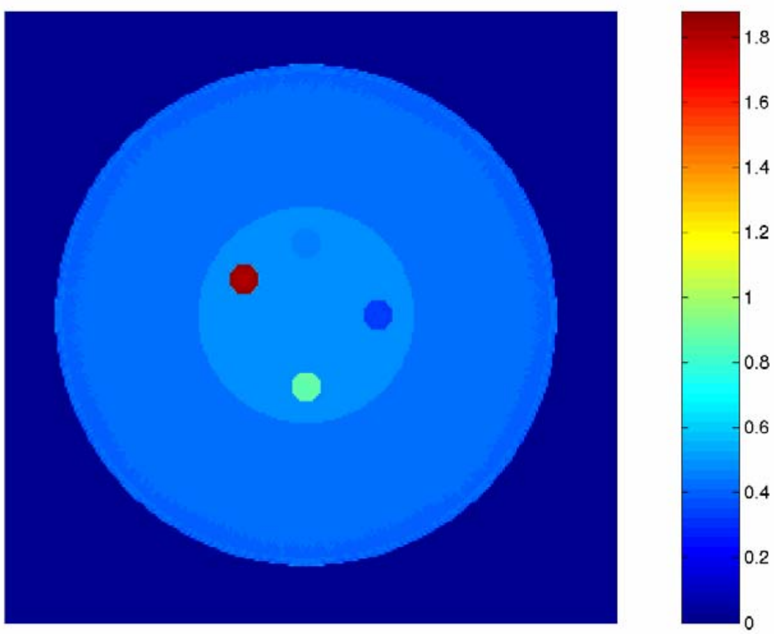

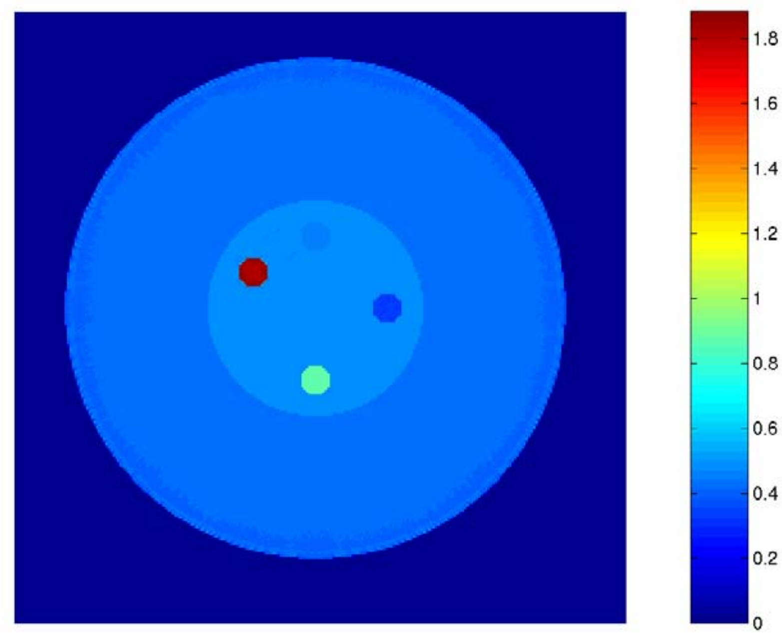

AM performance with multi-component tissue model

$$\hat{\mu}^{(100)}(x,E) \quad \text{vs.} \quad \mu(x,E)$$

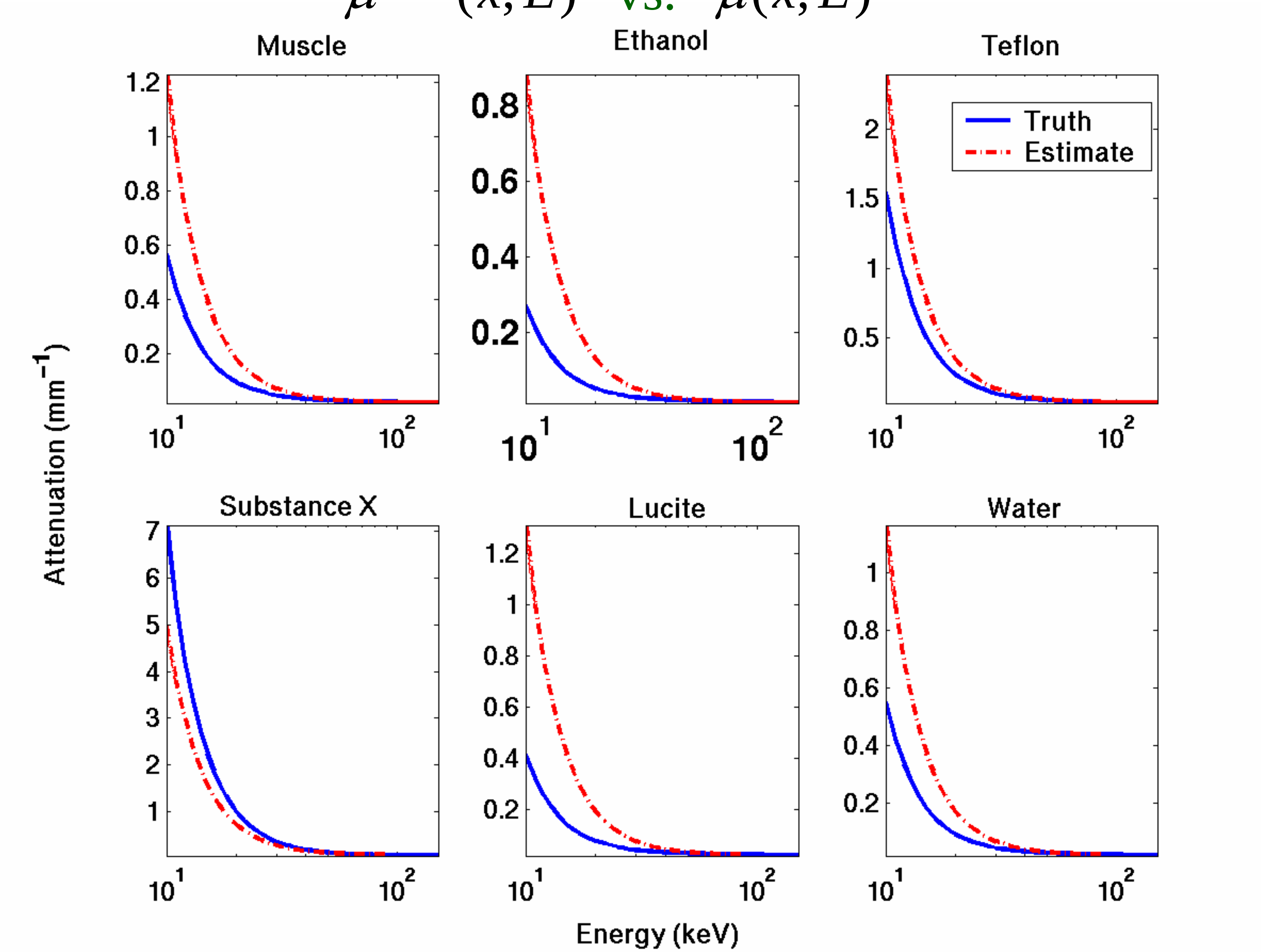

Dual Energy AM Algorithm

$$g_j(y) = \sum_E I_{0j}(y,E)\exp\left[-\sum_X h(y|x)\mu(x,E)\right] + \beta_j(y)\ ;\ j \in \{1,2\}$$

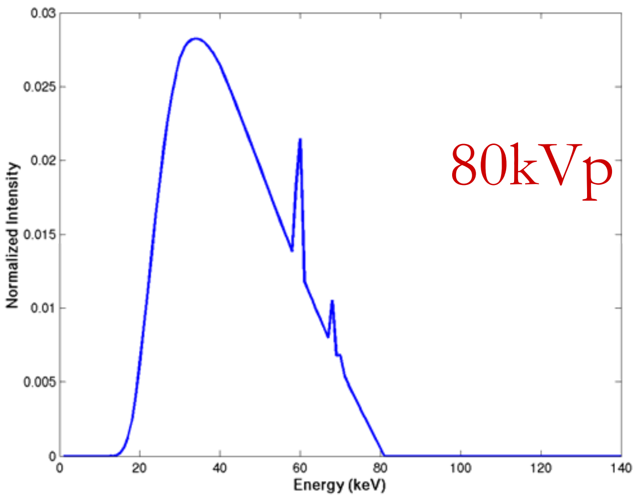

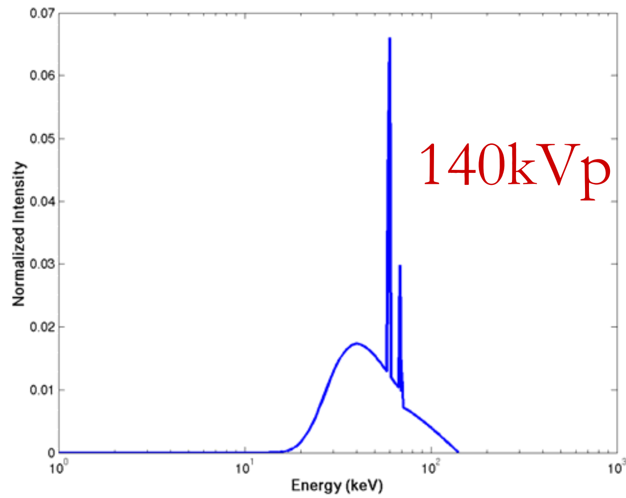

AM-DE update step: $$\hat{c}_i^{(k+1)} = \hat{c}_i^{(k+1)}(x) - \frac{1}{Z_i(x)} \ln\left(\frac{\sum_j \tilde{b}_{ij}^{(k)}(x)}{\sum_j \hat{b}_{ij}^{(k)}(x)} \right)$$

Alternative Dual Energy methods

Basis Vector Model (BVM)* → ESSRL Implementation

reconstructed values

$$\begin{bmatrix} \mu_x^{(1)} \\ \mu_x^{(2)} \end{bmatrix} = \underbrace{\begin{bmatrix} \mu_1^{(1)} & \mu_2^{(1)} \\ \mu_1^{(2)} & \mu_2^{(2)} \end{bmatrix}}_{\text{pre-computed}} \begin{bmatrix} c_1 \\ c_2 \end{bmatrix}$$

unknown coefficients

Calibration phantom:

- 2 water
- styrene
- $CaCl_2$

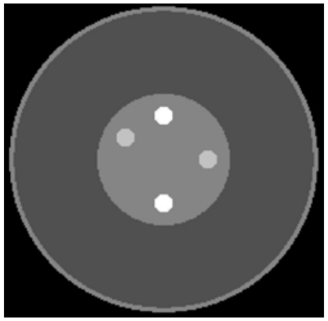

FBP

AM1

$$\begin{bmatrix} \mu_1^{(1)} & \mu_2^{(1)} \\ \mu_1^{(2)} & \mu_2^{(2)} \end{bmatrix}$$

*On Two-Parameter Representations of Photon Cross Sections: Application to Dual Energy CT imaging, Williamson, et al.

AMDE experiment results

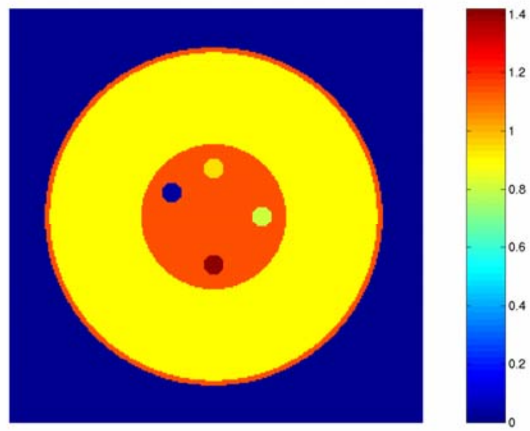

Noiseless data

200 iterations (22OS)

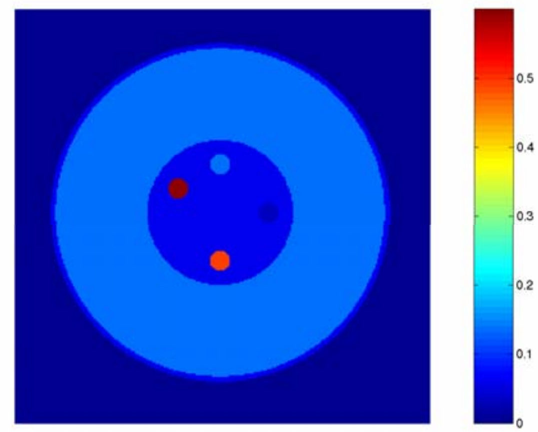

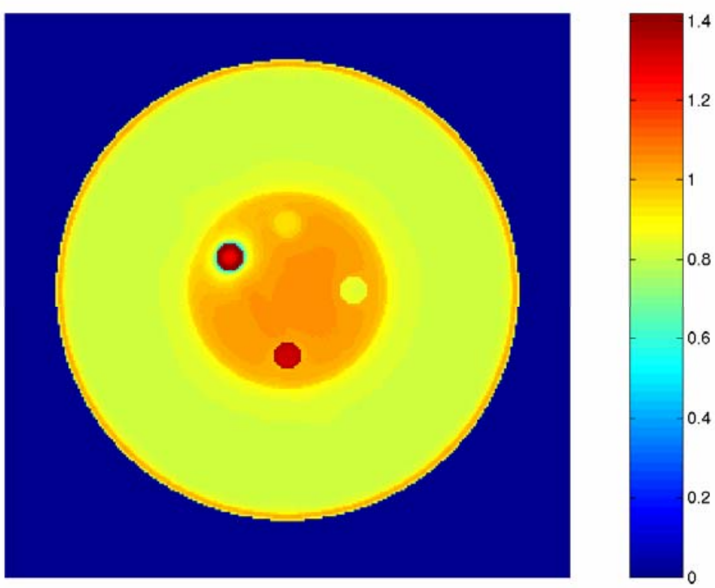

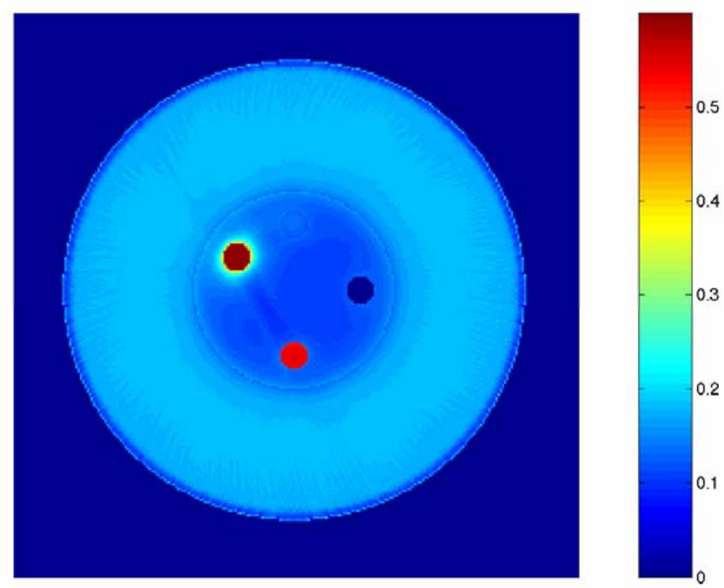

AMDE experiment results

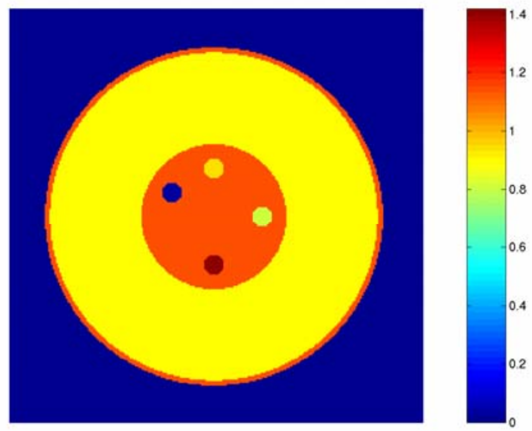

Noiseless data

1000 iterations (22OS)

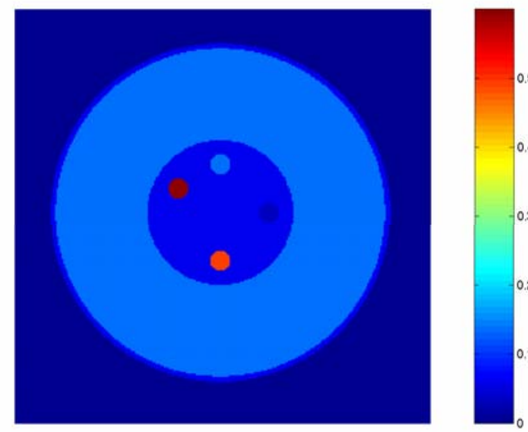

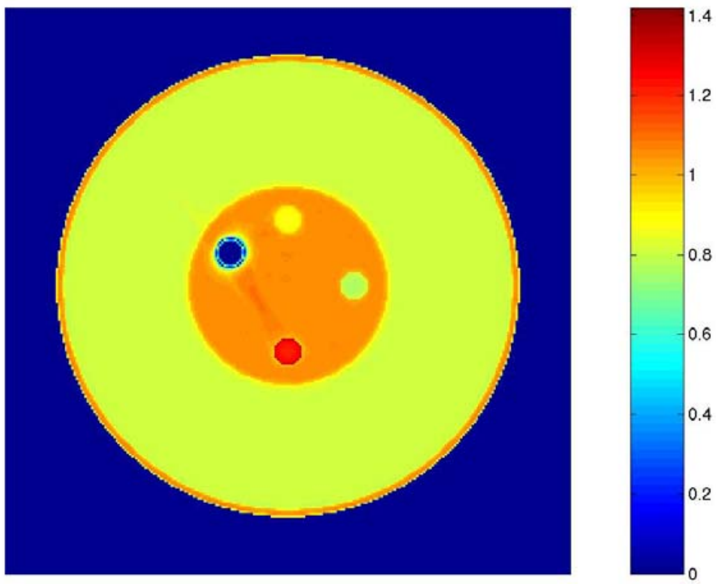

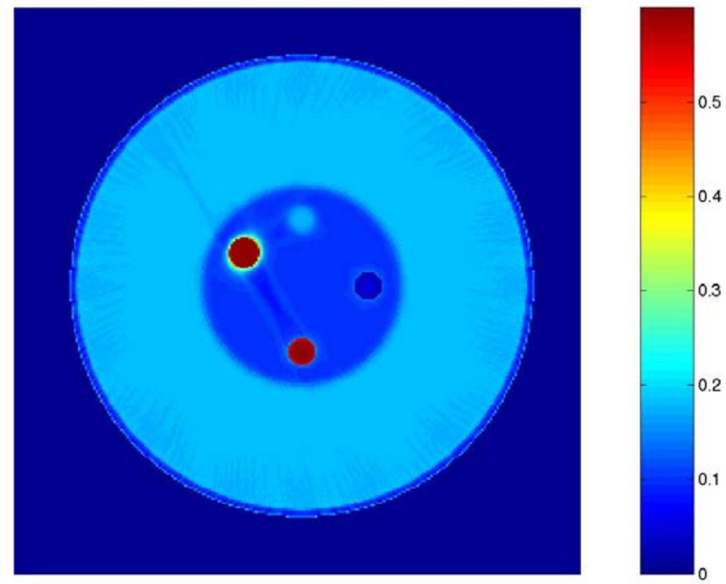

AMDE experiment results

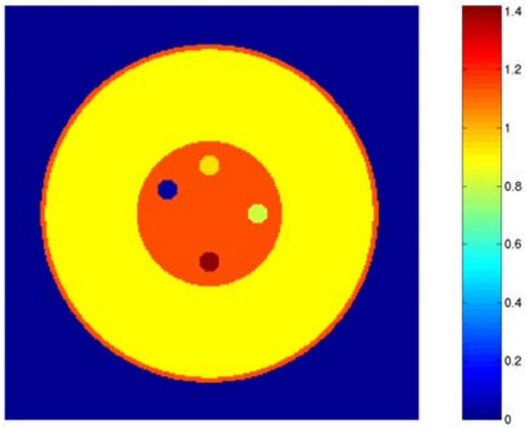

Noiseless data

2000 iterations
(22OS)

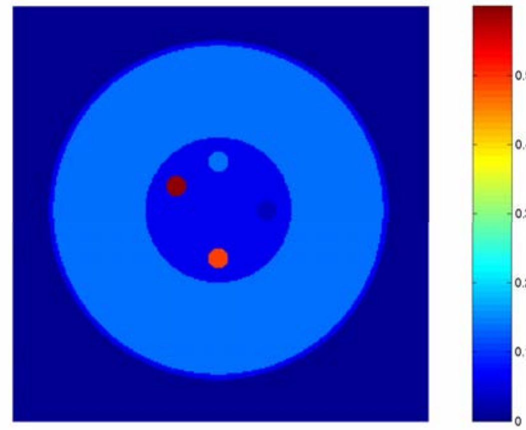

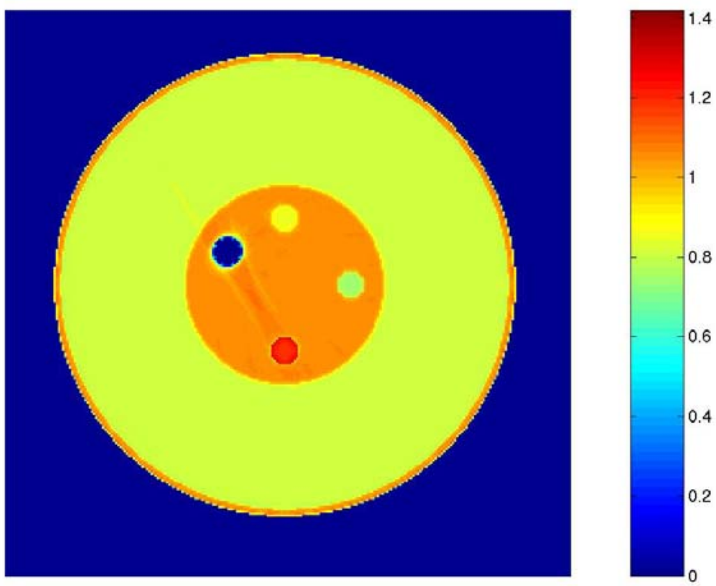

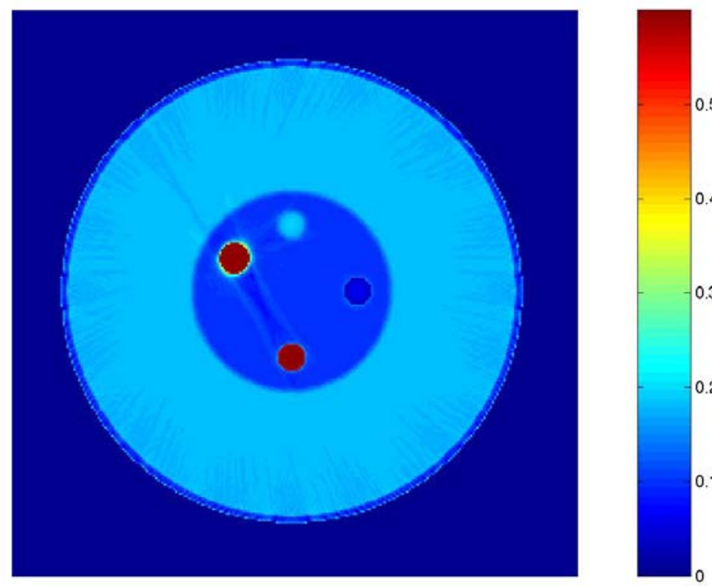

Relative error (%) in component images

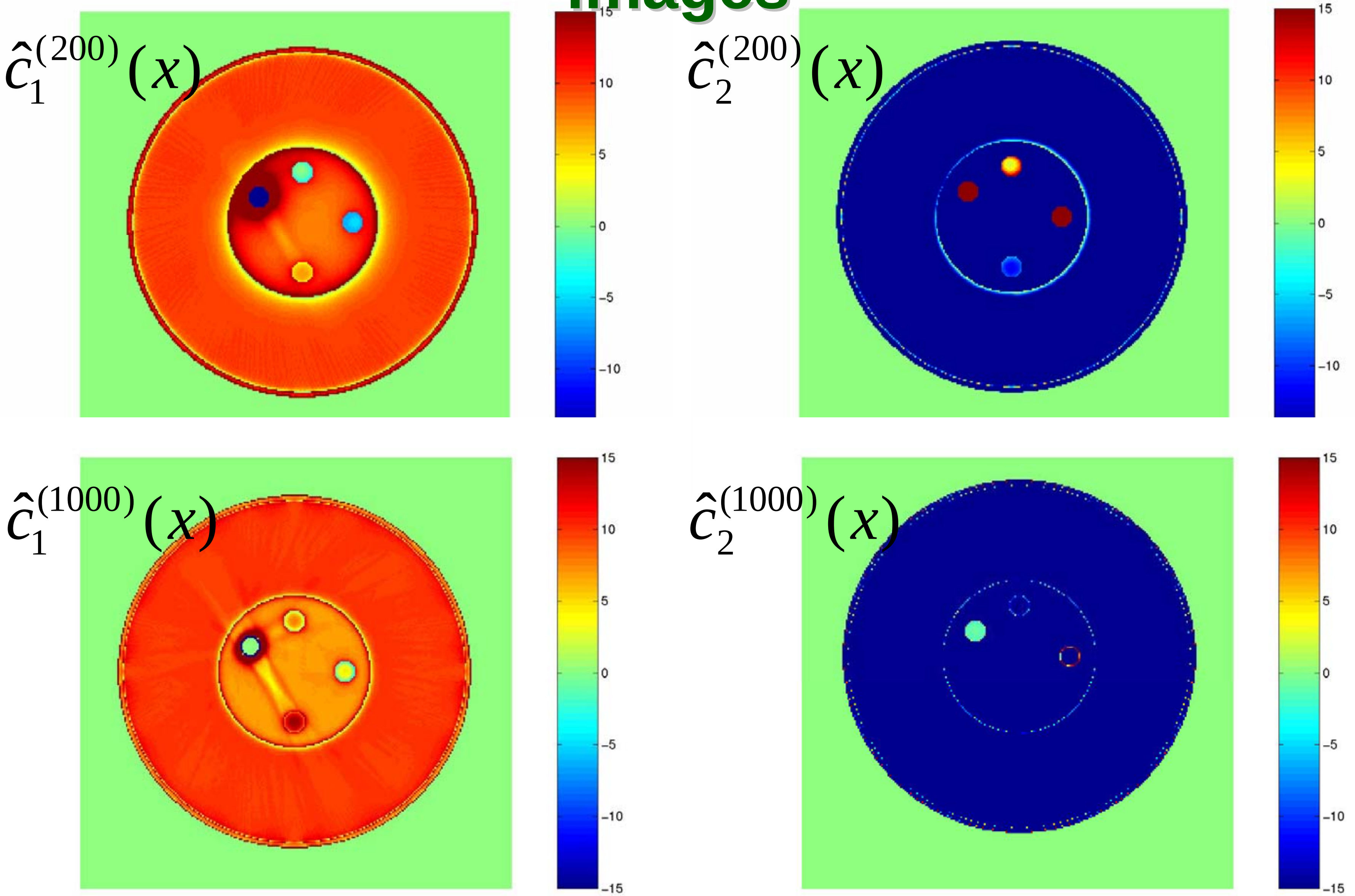

Relative error (%) in component images

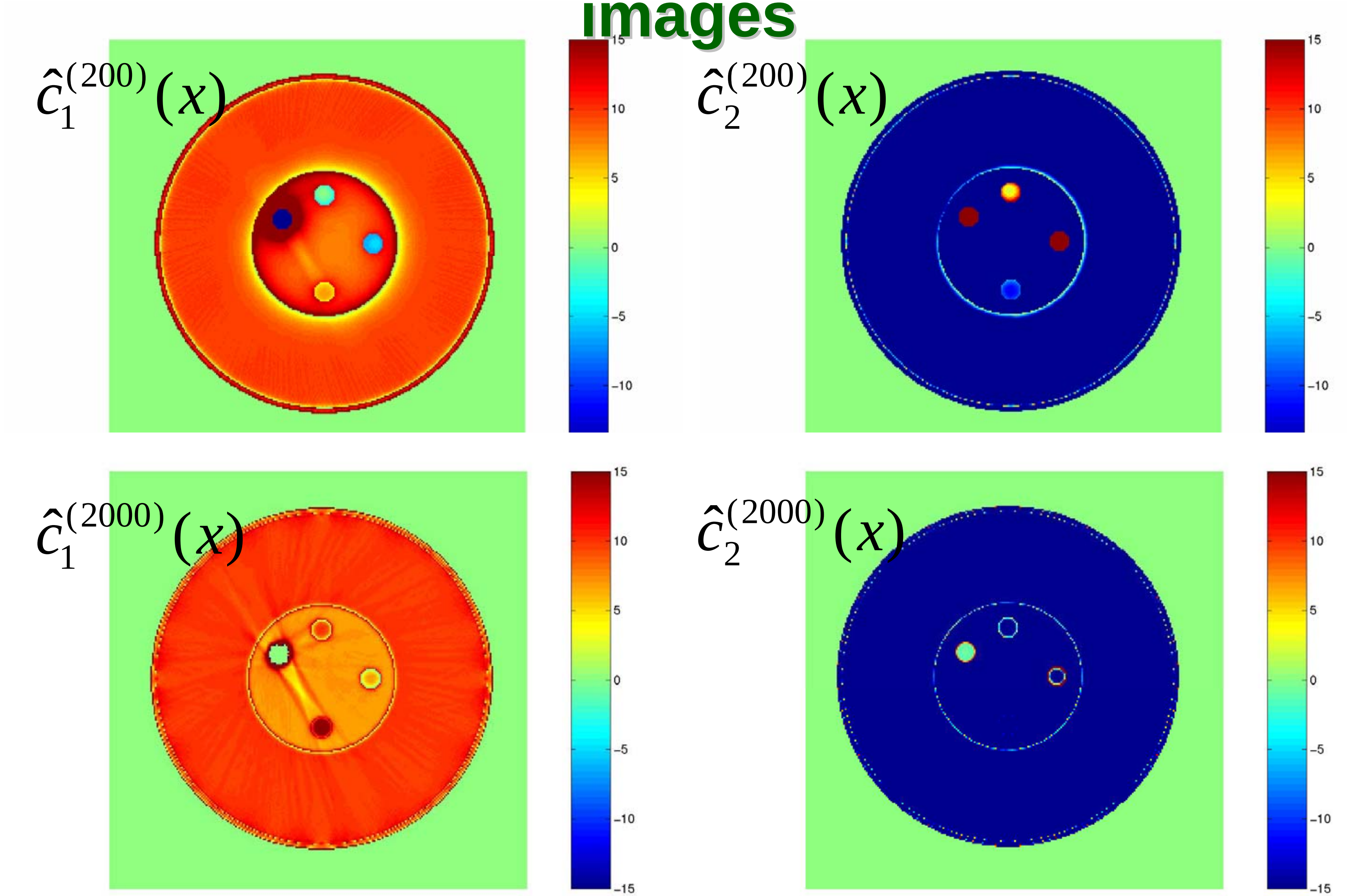

AMDE experiment results

Relative error vs. iteration

$$\hat{\mu}^{(200)}(x,E)$$

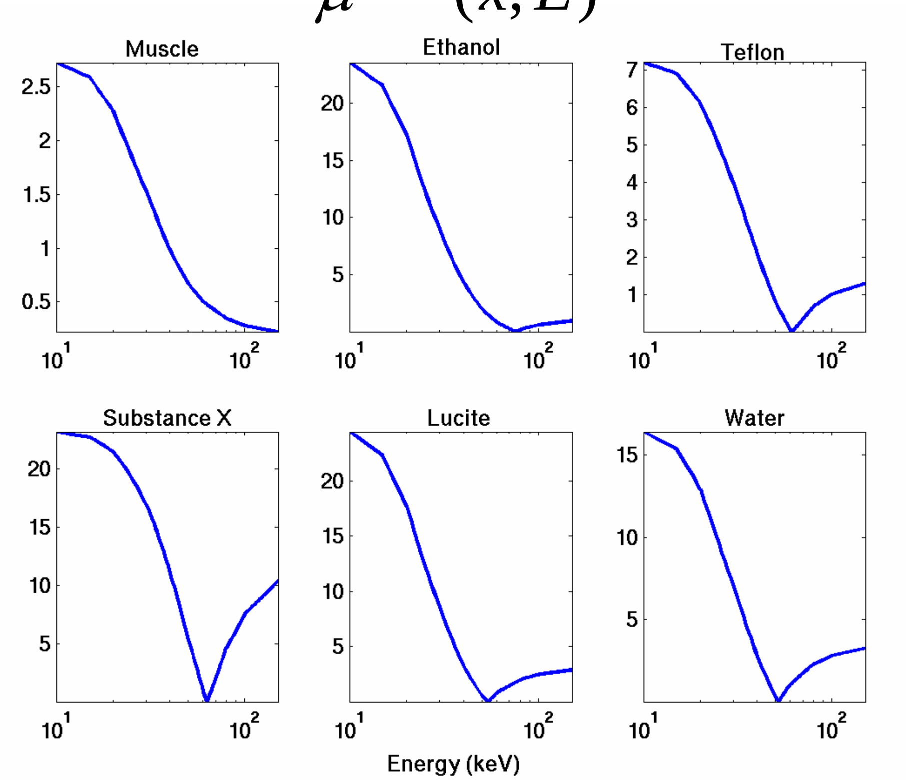

$$\hat{\mu}^{(1000)}(x,E)$$

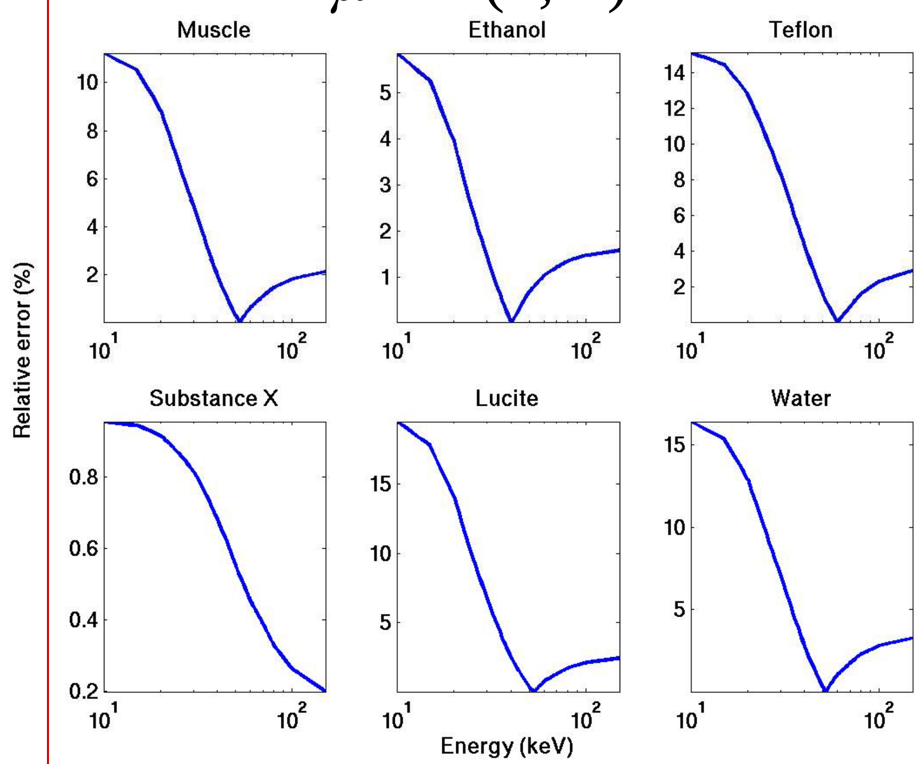

AMDE experiment results

Cost function vs. iteration

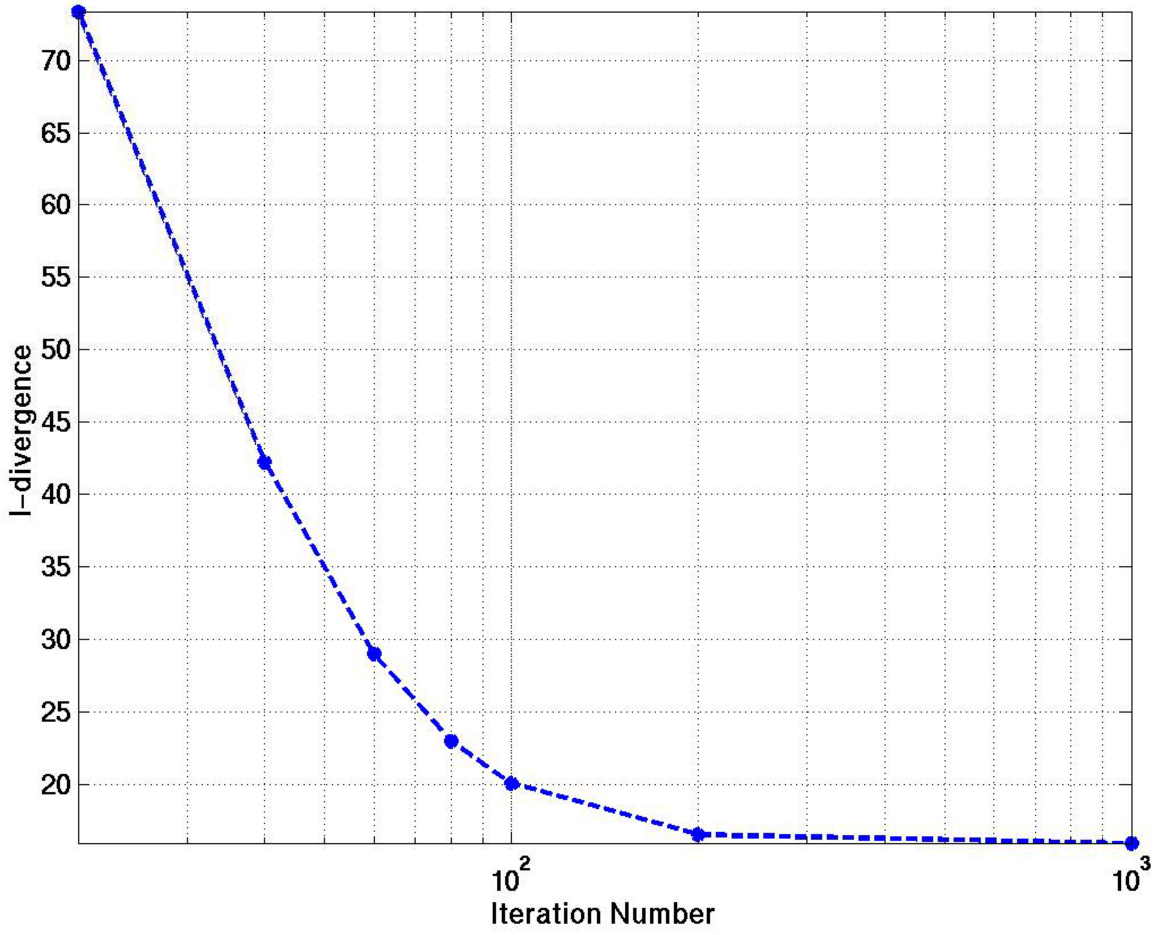

Alternative Method experiment results

BVM-FBP

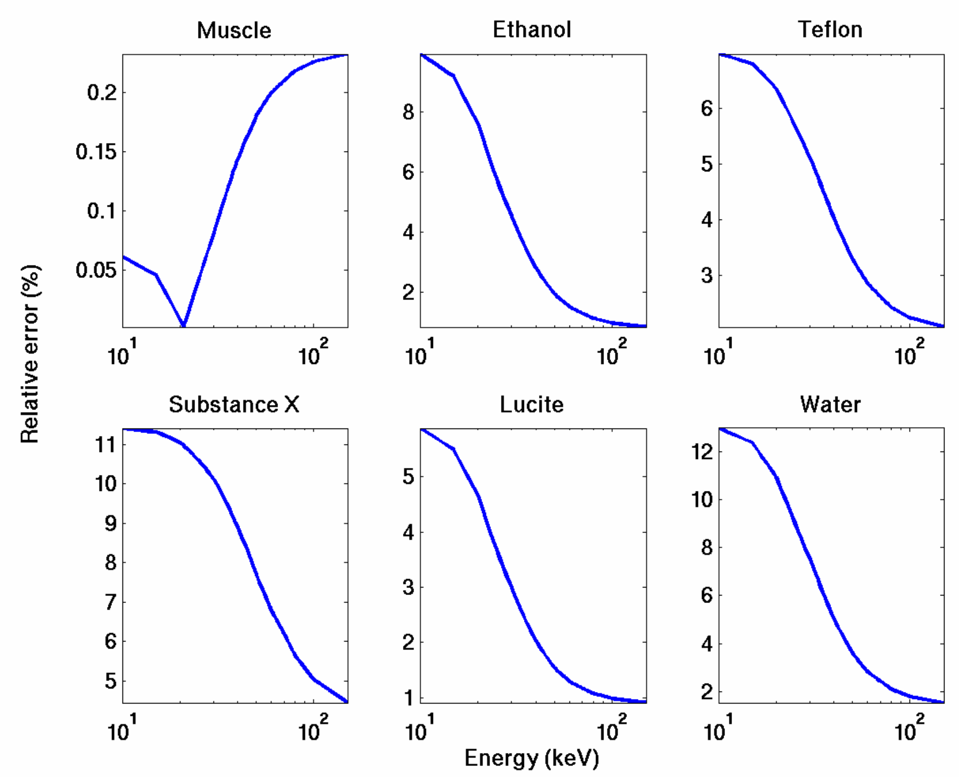

BVM-AM1

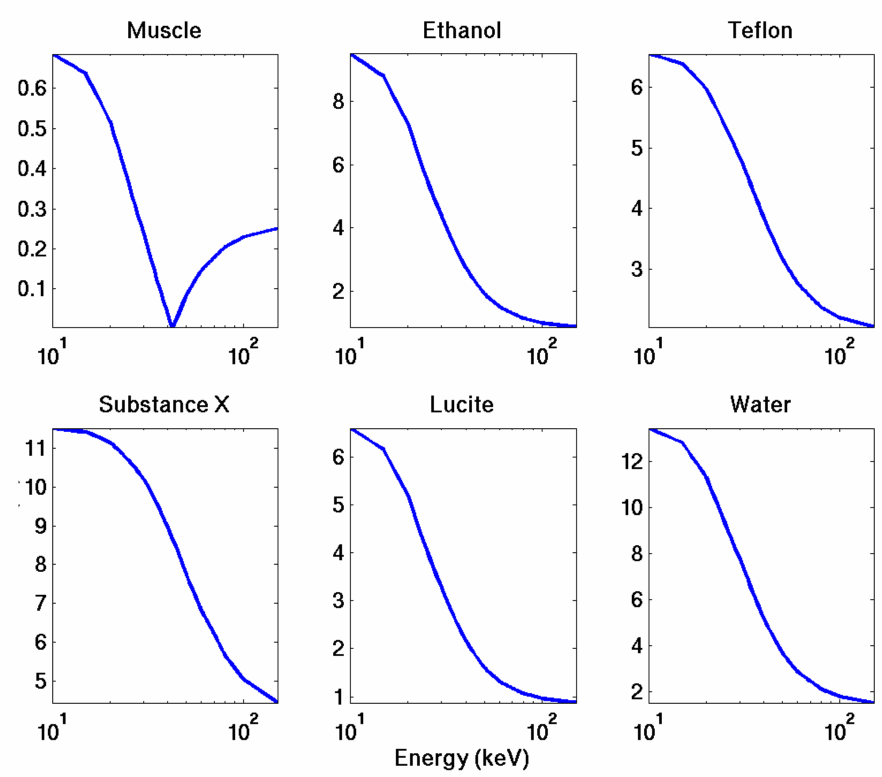

Data with noise
AMDE results

200 (22OS) iterations

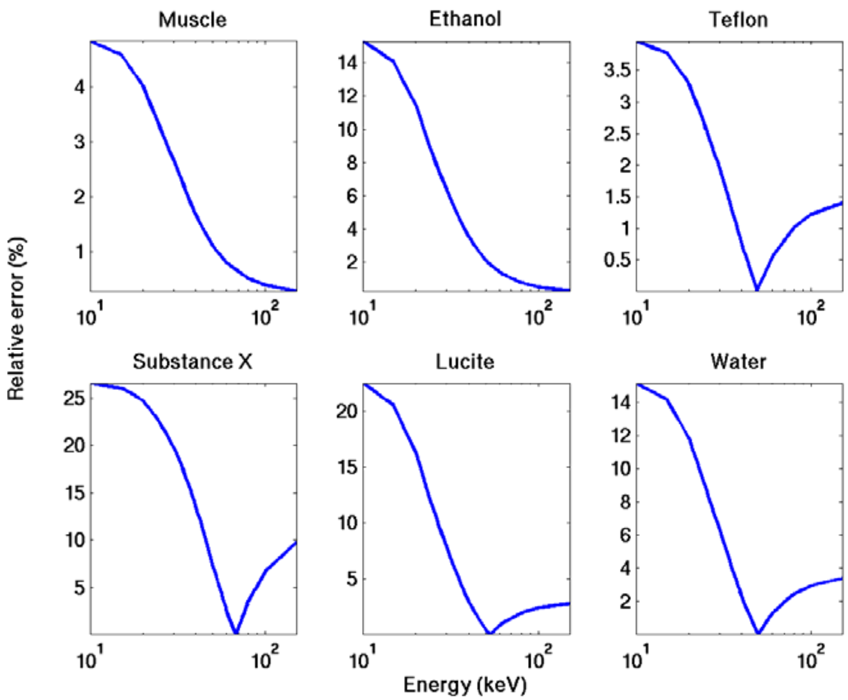

1000 (22OS) iterations

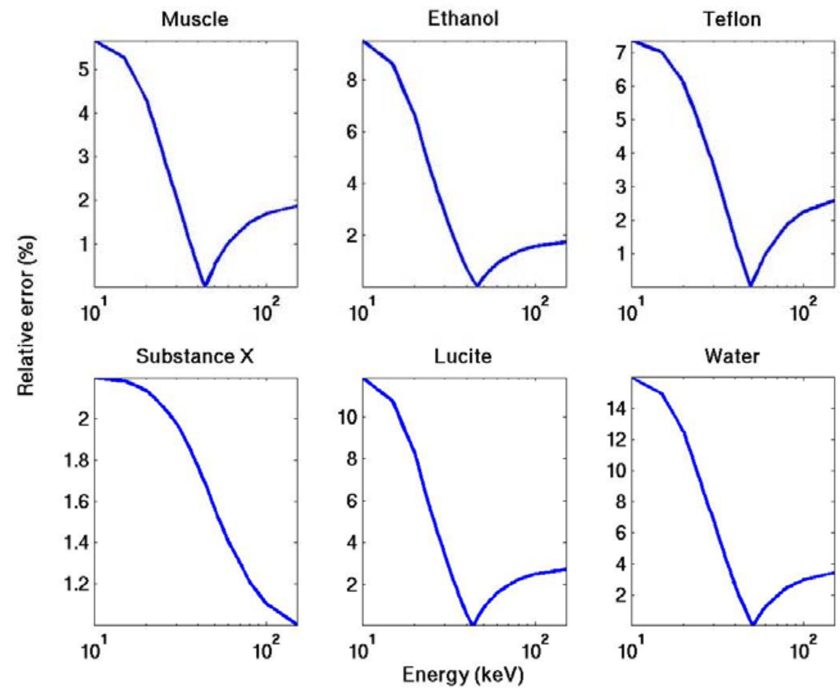

Data with noise
Alternative method results

BVM-FBP

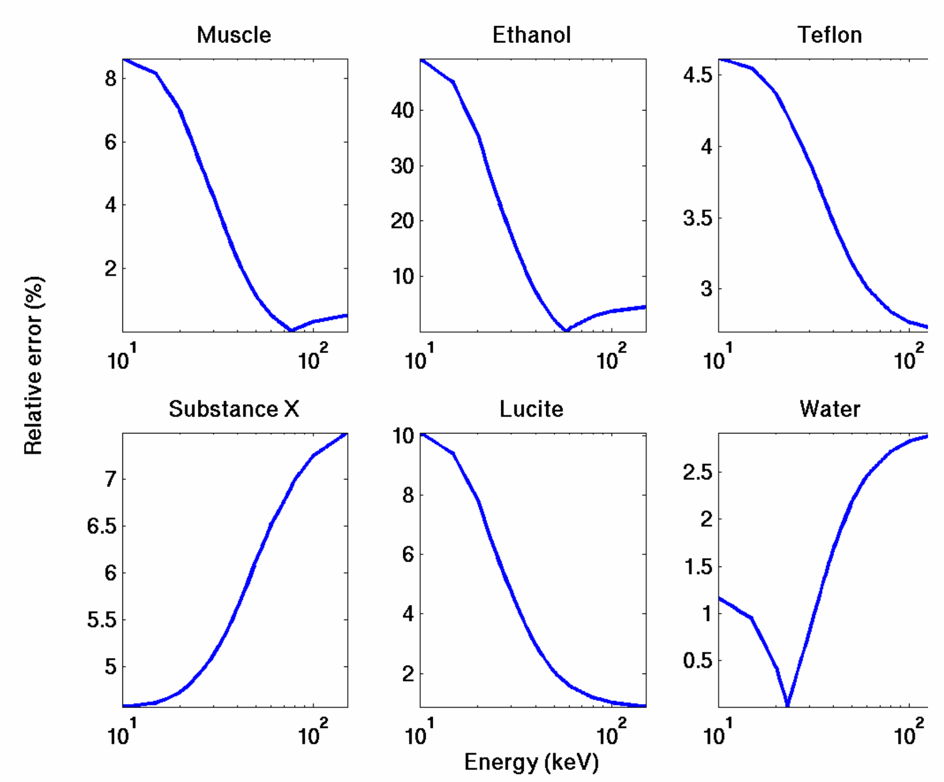

BVM-AM1

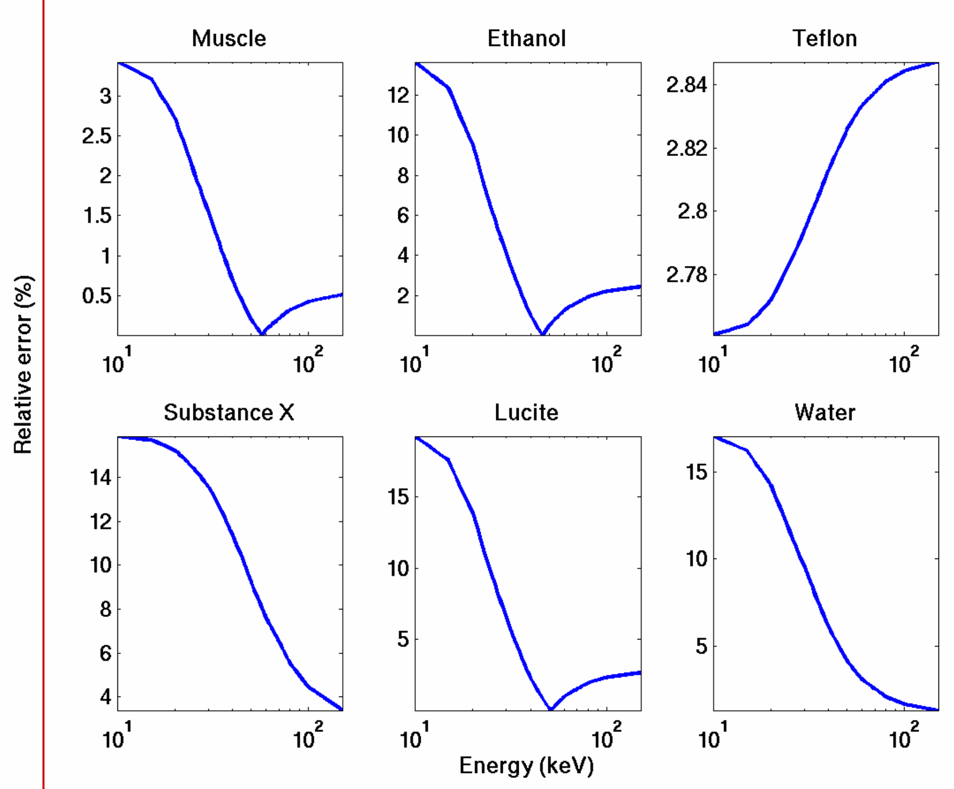

Conclusions

- X-Ray CT Imaging
- Likelihood Problem Formulation
- Information Geometry
- Alternating Minimization Algorithms
- Recent Progress: Limited Angle Tomography
- In Progress: 3D, Increased Convergence Rate, Dual Energy

Increased Convergence Rates

- Ordered subsets
  - Hudson and Larkin; Kamphuis and Beekman; etc.
- Separable Parabaloidal Surrogate functions
  - Fessler, et al.
- Multigrid Methods
  - Bouman, et al., 2001-2003
- Fast forward/backward projections
  - Bresler, et al.
- Other (see Sotthivirat, Ahn, Fessler, 2001-2003)

Multigrid Approach

Oh, Milstein, Bouman, Webb, et al.

- Objective functions at multiple grids
- Surrogate function view: match value and gradient at current estimate

$$\mathrm{cost}^{(m+1)}(x^{(m+1)})\Big|_{x^{(m+1)}=J_m^{m+1}x^{(m)}} = \mathrm{cost}^{(m)}(x^{(m)})$$

$$\nabla\mathrm{cost}^{(m+1)}(x^{(m+1)})\Big|_{x^{(m+1)}=J_m^{m+1}x^{(m)}} = \nabla\mathrm{cost}^{(m)}(x^{(m)})J_{m+1}^{m}$$

- Our implementations: little speedup; not matched to AM approach (not monotonic); negative values in estimates inside of logarithms

Multigrid AM Algorithm

Approach: compute image correction, $\Delta c(x)$, on coarse grid using AM

$$c(x) = c_{[0]}(x) + \Delta c(x)$$

$$\Delta c(x) = J_m^0 \Delta c_{[m]}(x)$$

$m = 0$	Fine grid
J_m^0	Interpolating operator

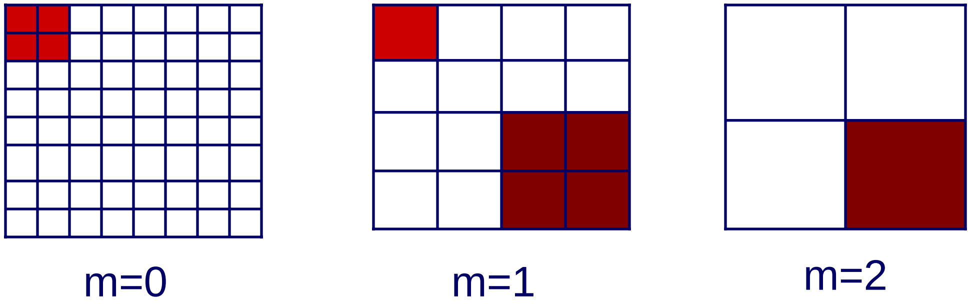

Multigrid AM Algorithm

$$\min_{q} \min_{p \in \mathcal{L}} I(p \| q) = \sum_{y \in \mathrm{Y}} \sum_{E} p(y,E) \ln \frac{p(y,E)}{q(y,E)} - p(y,E) + q(y,E)$$

$$q(y,E) = I_0(y,E) \exp\left(-\sum_{x \in \mathrm{X}} h(y,x) \sum_{i=1}^{N} \mu_i(E) \left[c_{i,[0]}(x) + J_m^0 \Delta c_{i,[m]}(x) \right] \right)$$

Comments:

- monotonicity guaranteed
- faster computations on coarser grids
- flexible grid sequence

Multigrid AM Algorithm
Iteration overview

On each grid *m*, run K_m iterations:

$$\hat{\Delta} c_{[m]}^{(k_m+1)}(x) = \hat{\Delta} c_{[m]}^{(k_m)}(x) - \frac{1}{Z_m(x)} \ln\left(\frac{b_m(x)}{\hat{b}_{[m]}^{(k_m)}(x)} \right), \qquad k_m = 0, \ldots, K_m - 1$$

$$b_{[m]}(x) = \sum_y d(y) h(y,x) J_m^0$$

$$\hat{b}_{[m]}^{(k_m)}(x) = \sum_y \hat{q}^{(k)}(y) \exp\left(-\sum_{x'} h(y,x') J_m^0 \hat{\Delta} c_{[m]}^{(k_m)}(x') \right) h(y,x) J_m^0$$

$$\hat{q}^{(k)}(y) = I_0(y) \exp\left(-\sum_x h(y,x) \hat{c}^{(k)}(x) \right)$$

Fine grid image update: $$\hat{c}^{(k+1)}(x) = \hat{c}^{(k)}(x) + J_m^0 \hat{\Delta} c_{[m]}^{(K_m)}(x)$$

Preliminary Results

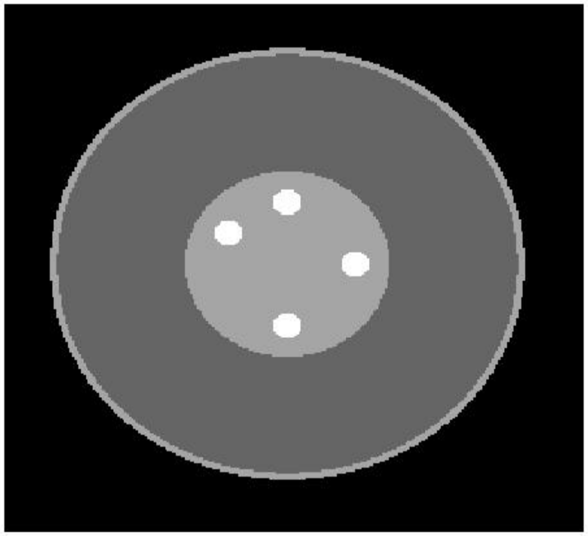

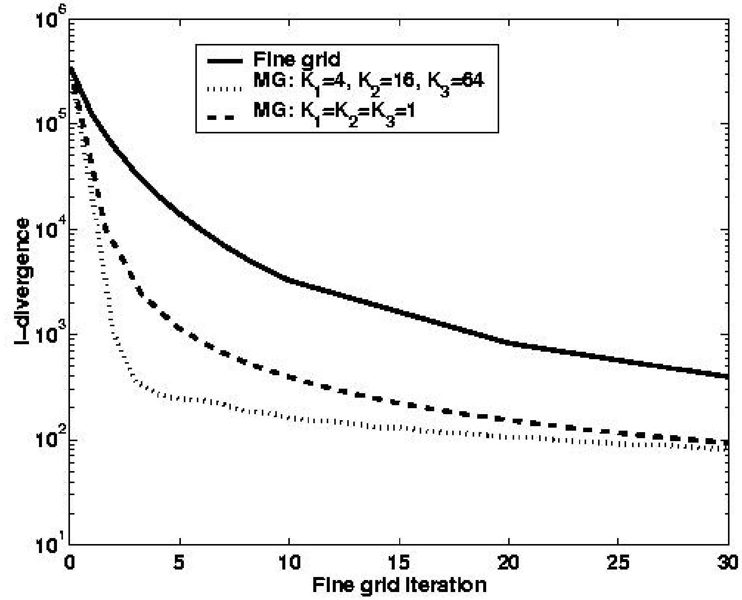

Simulated data:

- Lucite core in water bath with four metallic inserts
- 4 grid levels
- Interpolation – average of four neighbors

Comment: potential mismatch in projection operators

Conclusions and Future Work

- Multigrid Alternating Minimization Algorithm
  - potential for increasing convergence rate of single grid AM
  - guaranteed monotonic convergence properties
- Future analysis
  - Decimation operators in image space
  - Incorporate decimation in measurement space
  - Ordered subsets and multigrid combined

References

- J. A. O'Sullivan and J. Benac, "Alternating minimization algorithms for transmission tomography," submitted to *IEEE Trans. Med. Img*.
- S. Oh, B. Milstein, C. A. Bouman, K. J. Webb, "Adaptive nonlinear multigrid inversion with applications to Bayesian optical diffusion tomography," in *Proc. IEEE Stat. Signal Processing Workshop*, 2003
- T.-S. Pan, A. E. Yagle, "Numerical study of multigrid implementations of some iterative image reconstruction algorithms," in *Proc. IEEE Nuclear Sci. Symposium and Med. Img. Conference*, 1991.
- Z. Wu, A. H. Tewfik, "Multigrid algorithm for image reconstruction from Fourier modulus," in *Proc. ICASSP*, 1991.